Antenna Coding Empowered by Pixel Antennas

Shanpu Shen, *Senior Member, IEEE*, Kai-Kit Wong, *Fellow, IEEE*, and Ross Murch, *Fellow, IEEE*

Abstract—Pixel antennas, based on discretizing a continuous radiation surface into small elements called pixels, are a flexible reconfigurable antenna technology. By controlling the connections between pixels via switches, the characteristics of pixel antennas can be adjusted to enhance the wireless channel. Inspired by this, we propose a novel technique denoted antenna coding empowered by pixel antennas. We first derive a physical and electromagnetic based communication model for pixel antennas using microwave multiport network theory and beamspace channel representation. With the model, we optimize the antenna coding to maximize the channel gain in a single-input single-output (SISO) pixel antenna system and develop a codebook design for antenna coding to reduce the computational complexity. We analyze the average channel gain of SISO pixel antenna system and derive the corresponding upper bound. In addition, we jointly optimize the antenna coding and transmit signal covariance matrix to maximize the channel capacity in a multiple-input multiple-output (MIMO) pixel antenna system. Simulation results show that using pixel antennas can enhance the average channel gain by up to 5.4 times and channel capacity by up to 3.1 times, demonstrating the significant potential of pixel antennas as a new dimension to design and optimize wireless communication systems.

Index Terms—Antenna coding, beamspace, binary optimization, capacity, channel gain, codebook, MIMO, pixel antenna.

I. INTRODUCTION

ANTENNAS play a significant role in wireless communication systems. Utilizing multiple antennas, multiple-input multiple-output (MIMO) systems have been one of the most celebrated wireless communication technologies over the past few decades. It has evolved from point-to-point MIMO in the third generation (3G) to multiuser MIMO in the fourth generation (4G) and massive MIMO in the fifth generation (5G), and will still be a dominating technology in the upcoming sixth generation (6G) [1]. However, the antennas utilized in conventional MIMO technologies have fixed configurations and characteristics such as operating frequency, radiation pattern, and polarization, which are not involved in the signal processing and system optimization in wireless communications. As 6G mobile communication strives to push

S. Shen is with the State Key Laboratory of Internet of Things for Smart City and Department of Electrical and Computer Engineering, University of Macau, Macau, China (email: shanpushen@um.edu.mo).

K. K. Wong is affiliated with the Department of Electronic and Electrical Engineering, University College London, Torrington Place, WC1E 7JE, United Kingdom and he is also affiliated with Yonsei Frontier Lab, Yonsei University, Seoul, Korea (e-mail: kai-kit.wong@ucl.ac.uk).

R. Murch is with the Department of Electronic and Computer Engineering and the Institute of Advanced Study, The Hong Kong University of Science and Technology, Clear Water Bay, Kowloon, Hong Kong (e-mail: eermurch@ust.hk).

the performance to extreme levels far beyond current 5G mobile communications, it is necessary to seek a paradigm shift in antenna technology to achieve a new degree of freedom in designing and optimizing wireless communication systems, so as to break through the current performance limit.

Pixel antennas are a flexible antenna technology to design highly reconfigurable antennas and dates back to 2004 [2], [3]. The concept of the pixel antenna is based on discretizing a continuous radiation surface into small elements, which are referred to as pixels, and connecting adjacent pixels through hardwires or RF switches [4], [5], [6], [7], [8], [9] and [10]. By controlling the connections between pixels, various antenna topologies can be formed so that the pixel antenna can be reconfigured to achieve a wide range of distinct antenna characteristics such as operating frequency, radiation pattern, and polarization. For example, a frequency-reconfigurable pixel antenna, which can reconfigure the operating frequency from PCS band to UMTS band, has been designed in [7], and pattern-reconfigurable pixel antennas, which can reconfigure the radiation pattern to implement 360° single- or multi-beam steering, have been designed in [8], [9], and [10]. Moreover, various pixel antennas have been designed for different applications. In [11], a reconfigurable intelligent surface with pixelated elements, which can reconfigure the phase shift of reflected waves, has been designed. In [12], and [13], multiport pixel rectennas, which can maximize the output dc power for ambient RF energy harvesting, have been developed. In [14], MIMO antennas with pixelated surface, which provide low mutual coupling and spatial correlation to maximize the ergodic capacity, have been developed. In [15], defected ground structures with pixelated grid, which suppress cross-polarization and achieve circular polarization, have been designed. While these works [3], [4], [5], [6], [7], [8], [9], [10], [11], [12], [13], [14], [15] have designed pixel antennas with significant performance enhancement, the investigations are limited at the level of antenna hardware design and do not consider the impact on wireless communications at the level of the system. Thus, it is necessary to explore using pixel antennas to design and optimize wireless communication systems.

In parallel with the development of pixel antennas, the concept of the fluid antenna system (FAS) has also been proposed and introduced in 2020 [16]. FAS originated from the emergence of mechanically flexible antennas such as liquid antennas based on liquid metals or ionized solutions [17], which enables a single antenna freely switching the position in a small linear space. Moreover, FAS can be implemented by any appropriate reconfigurable technique including electronically flexible pixel antennas, where the pixels can be turned on-and-off instantly so that several pixels can be turned on to form an antenna port in a particular position. One of the first pixel

antenna designs for an FAS has been demonstrated in [18] to show that a single pixel antenna can mimic switching positions in a small linear space and be useful for FAS. Leveraging the position-switchable property, FAS can select the optimal position in a given space to adapt to fading channels [19] and thus enhance the system performance such as level crossing rate [16], diversity gain [20], and outage probability [21]. FAS has also been utilized to assist MIMO communication systems [22], [23], [24], [25]. Specifically, the capacity, diversity-multiplexing tradeoff, spectral efficiency, and energy efficiency for MIMO-FAS have been investigated in [22], [23], [24] and the rate maximization for MIMO-FAS based on statistical channel state information (CSI) has been studied in [25]. In addition, a novel multiple access based on FAS, denoted as fluid antenna multiple access (FAMA), has been proposed in [26], and FAMA can be categorized into fast FAMA [27] and slow FAMA [28], Moreover, FAS has been investigated to enhance emerging areas such as secret communications [29] and full duplex communications [30].

While the emergence and development of FAS [16], [19], [20], [21], [22], [23], [24], [25], [26], [27], [28], [29], [30] has preliminarily demonstrated the potential of pixel antennas for designing and optimizing wireless communication system, there is much further potential for pixel antennas to be exploited in wireless communication. For example, utilizing the individual pixels inside a pixel antenna, and the connections between them, can open up new possibilities for their use in wireless communication. To fully exploit the potential of pixel antennas for wireless communication, there remains two open problems: 1) how to derive a physical and electromagnetic (EM) based communication model for pixel antennas, and 2) how to efficiently utilize the flexibility of pixel antennas to enhance wireless communications.

In this paper, we propose using pixel antennas to enhance wireless communication systems with an EM based model and a systematic and efficient approach. In comparison with conventional wireless communication systems using antennas with fixed configuration, using pixel antennas allows designing and optimizing wireless communication systems in a new dimension through adjusting the antenna configuration, and thus the wireless communication systems performance can be significantly enhanced. The contributions of the paper are summarized as follows.

First, we propose a novel technique called *antenna coding* empowered by pixel antennas to enhance wireless communication systems. By adjusting the connections between adjacent pixels through switches, the characteristics of the pixel antenna such as impedance, radiation pattern, and polarization can be controlled. Inspired by this, we propose antenna coding, which is a technique to control antenna configuration and characteristics through binary codes representing switches for enhancing wireless systems. With antenna coding, wireless systems can be optimized with a new dimension and thus achieve enhanced performance compared to conventional systems with fixed antenna configuration.

Second, we derive a physical and EM based model for pixel antennas. Using microwave multiport network theory, we analyze the pixel antenna and model its configuration and characteristics such as radiation pattern as functions of a binary vector referred to as the *antenna coder* which represents the switch on and off states. Further, using the beamspace channel representation, we incorporate radiation patterns into the channel to derive a communication model for pixel antennas, where the channel can be controlled by antenna coder, allowing antenna coding optimization to enhance wireless systems.

Third, we optimize the antenna coding to maximize the channel gain in single-input single-output (SISO) pixel antenna systems. The antenna coding optimization is a binary optimization problem and can be solved by a successive exhaustive Boolean optimization approach. To reduce the computational complexity for optimization, we propose a codebook design for antenna coding and optimize the antenna coder by searching the codebook.

Fourth, we analyze the average channel gain of SISO pixel antenna systems and find that the upper bound of average channel gain is the effective aerial degrees-of-freedom of pixel antennas which can be found by singular value decomposition of the open-circuit radiation pattern matrix.

Fifth, we jointly optimize the antenna coding and transmit signal covariance matrix to maximize the channel capacity in MIMO pixel antenna systems by using exhaustive Boolean optimization approach and searching of the codebook design.

Sixth, we evaluate the performance of SISO and MIMO pixel antenna systems compared to conventional SISO and MIMO systems using antennas with fixed configuration. The simulation results show that using pixel antennas can enhance the average channel gain by up to 5.4 times and the channel capacity by up to 3.1 times, demonstrating the significant potential of pixel antennas in wireless communication systems.

Organization: Section II introduces the pixel antenna model and antenna coding. Section III presents the SISO pixel antenna system and antenna coding design for channel gain maximization. Section IV presents the MIMO pixel antenna system and antenna coding design for capacity maximization. Section V provides performance evaluation for the SISO and MIMO pixel antenna system. Section VI provides discussions and future work. Section VII concludes this work.

Notation: Bold lower and upper case letters represent vectors and matrices, respectively. A symbol without bold font denotes a scalar. $\mathbb{R}$ and $\mathbb{C}$ represent real and complex number sets, respectively. $\mathbb{E}\left[\cdot\right]$ denotes the expectation. $(\cdot)^{+}$ denotes the positive part. $|a|$ denotes the modulus of a complex number a. $[\mathbf{a}]_i$ and $\|\mathbf{a}\|$ denote the ith element and l_2-norm of a vector $\mathbf{a}$, respectively. $\mathbf{A}^*$, $\mathbf{A}^T$, $\mathbf{A}^H$, $[\mathbf{A}]_{:,i}$, $[\mathbf{A}]_{i,j}$, $|\mathbf{A}|$, and $\text{Tr}\left(\mathbf{A}\right)$ denote the conjugate, transpose, conjugate transpose, ith column, (i,j)th element, determinant, and trace of a matrix $\mathbf{A}$, respectively. $\mathcal{CN}(\mathbf{0},\boldsymbol{\Sigma})$ denotes the circularly symmetric complex Gaussian distribution with mean $\mathbf{0}$ and covariance matrix $\boldsymbol{\Sigma}$. $\text{diag}\left(a_1,...,a_N\right)$ denotes a diagonal matrix with entries $a_1,...,a_N$. $\mathbf{I}$ denotes an identity matrix.

II. PIXEL ANTENNA

In this section, we introduce the pixel antenna model and the proposed antenna coding technique. As illustrated in the schematic in Fig. 1(a), the pixel antenna is based on discretizing a continuous radiation surface into small elements, which
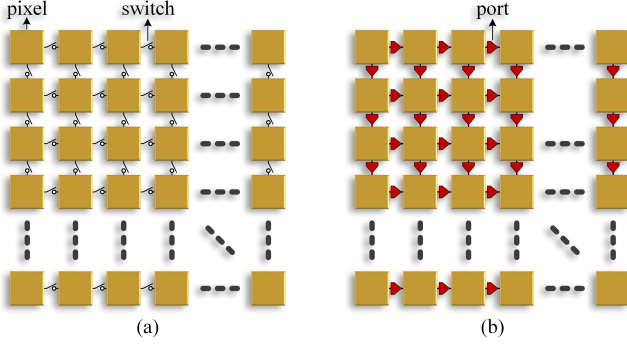
Fig. 1. (a) Schematic for pixel antenna. (b) Multiport circuit network for pixel antenna. Red arrows represent the ports which replace switches.
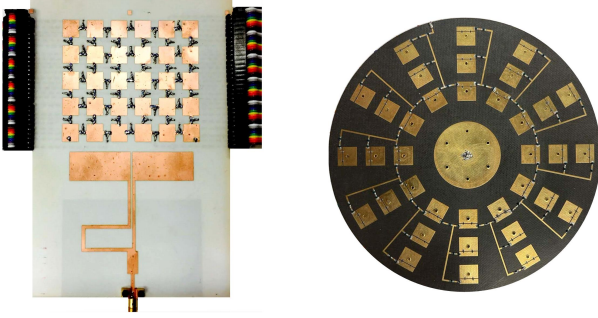

Fig. 2. Two examples of pixel antenna designs proposed in [8] and [10].

are referred to as pixels, and adjacent pixels can be connected through switches to flexibly control the antenna configuration and characteristics such as radiation pattern. Two examples of pattern-reconfigurable pixel antenna designs proposed in [8] and [10] are shown in Fig. 2.

The pixel antenna can be modeled using microwave multi-port network theory[1]. Specifically, considering a pixel antenna which has Q switches, we can model the pixel antenna as a multiport circuit network by replacing the Q switches with Q ports as shown in Fig. 1(b). Thus, the entire pixel antenna can be modeled as a $(Q+1)$-port circuit network, which consists of one antenna port and Q pixel ports denoting the connections between adjacent pixels (which are numbered 2 to $Q+1$), as shown in Fig. 3. The $(Q+1)$-port circuit network can be characterized by a $(Q+1) \times (Q+1)$ impedance matrix $\mathbf{Z}$, which can be partitioned as

$$\mathbf{Z} = \begin{bmatrix} z_{\mathrm{AA}} & \mathbf{z}_{\mathrm{AP}} \\ \mathbf{z}_{\mathrm{PA}} & \mathbf{Z}_{\mathrm{PP}} \end{bmatrix}, \quad (1)$$

where $z_{\mathrm{AA}} \in \mathbb{C}$ is the self impedance for the antenna port, $\mathbf{Z}_{\mathrm{PP}} \in \mathbb{C}^{Q \times Q}$ is the impedance matrix for the Q pixel ports, $\mathbf{z}_{\mathrm{AP}} \in \mathbb{C}^{1 \times Q}$ is the trans-impedance relating the voltage of the antenna port with currents of the Q pixel ports, and $\mathbf{z}_{\mathrm{PA}} \in \mathbb{C}^{Q \times 1}$ is the transpose of $\mathbf{z}_{\mathrm{AP}}$. We denote the voltages at the antenna port and pixel ports as $v_{\mathrm{A}} \in \mathbb{C}$

Fig. 3. Model of the multiport circuit network for pixel antenna.

and $\mathbf{v}_{\mathrm{P}} = [v_{\mathrm{P},1}, \ldots, v_{\mathrm{P},Q}] \in \mathbb{C}^{Q \times 1}$, respectively, and the currents at the antenna port and pixel ports as $i_{\mathrm{A}} \in \mathbb{C}$ and $\mathbf{i}_{\mathrm{P}} = [i_{\mathrm{P},1}, \ldots, i_{\mathrm{P},Q}] \in \mathbb{C}^{Q \times 1}$, respectively. Using (1), we can relate the voltages and currents by

$$\begin{bmatrix} v_{\mathrm{A}} \\ \mathbf{v}_{\mathrm{P}} \end{bmatrix} = \begin{bmatrix} z_{\mathrm{AA}} & \mathbf{z}_{\mathrm{AP}} \\ \mathbf{z}_{\mathrm{PA}} & \mathbf{Z}_{\mathrm{PP}} \end{bmatrix} \begin{bmatrix} i_{\mathrm{A}} \\ \mathbf{i}_{\mathrm{P}} \end{bmatrix}. \quad (2)$$

The switch connected to the qth pixel port has two states, on or off[2]. As shown in Fig. 3, we can model the switch as a load impedance $z_{\mathrm{L},q}\ \forall q$ with open or short circuit, i.e. $z_{\mathrm{L},q} = 0$ or ∞. Therefore, a binary variable $b_q \in \{0,1\}$ can be used to denote the state of the switch connected to the qth port, i.e.

$$z_{\mathrm{L},q} = \begin{cases} 0, & b_q = 0, \text{ i.e. switch on,} \\ \infty, & b_q = 1, \text{ i.e. switch off.} \end{cases} \quad (3)$$

Numerically, for the switch off state, we can set $z_{\mathrm{L},q}$ as a very large value, for example $z_{\mathrm{L},q} = 10^8$, to approach the infinite. We group $z_{\mathrm{L},q}\ \forall q$ into a diagonal load impedance matrix $\mathbf{Z}_{\mathrm{L}} = \mathrm{diag}(z_{\mathrm{L},1}, \ldots, z_{\mathrm{L},Q}) \in \mathbb{C}^{Q \times Q}$ and group $b_q\ \forall q$ into a vector $\mathbf{b} = [b_1, \ldots, b_Q]^T \in \mathbb{R}^{Q \times 1}$, which represents the states of all switches and is referred to as an antenna coder. Therefore, the load impedance matrix $\mathbf{Z}_{\mathrm{L}}$ can be coded by $\mathbf{b}$, denoted as $\mathbf{Z}_{\mathrm{L}}(\mathbf{b})$, so that $\mathbf{v}_{\mathrm{P}}$ and $\mathbf{i}_{\mathrm{P}}$ can be related by

$$\mathbf{v}_{\mathrm{P}} = -\mathbf{Z}_{\mathrm{L}}(\mathbf{b}) \mathbf{i}_{\mathrm{P}}. \quad (4)$$

Substituting (4) into (2), we can find that the currents at the pixel ports can be coded by the antenna coder $\mathbf{b}$, written as

$$\mathbf{i}_{\mathrm{P}}(\mathbf{b}) = -(\mathbf{Z}_{\mathrm{PP}} + \mathbf{Z}_{\mathrm{L}}(\mathbf{b}))^{-1} \mathbf{z}_{\mathrm{PA}} i_{\mathrm{A}}. \quad (5)$$

Accordingly, the radiation pattern of the pixel antenna can also be coded by the antenna coder $\mathbf{b}$. Given an antenna coder $\mathbf{b}$, we denote the radiation pattern of the pixel antenna excited by current i_{A} as $\mathbf{e}(\mathbf{b}) = [\mathbf{e}_\theta^T(\mathbf{b}), \mathbf{e}_\phi^T(\mathbf{b})]^T \in \mathbb{C}^{2K \times 1}$ where

---

[1]The multiport circuit network model can be traced back to the method of moments (MoM) [31] which uses an impedance matrix to model an antenna. Using multiport circuit network to model lumped elements, such as capacitor, inductor, resistor, and RF switches, has been developed and demonstrated in [32], [33] and verified in reconfigurable antenna designs [7], [34].
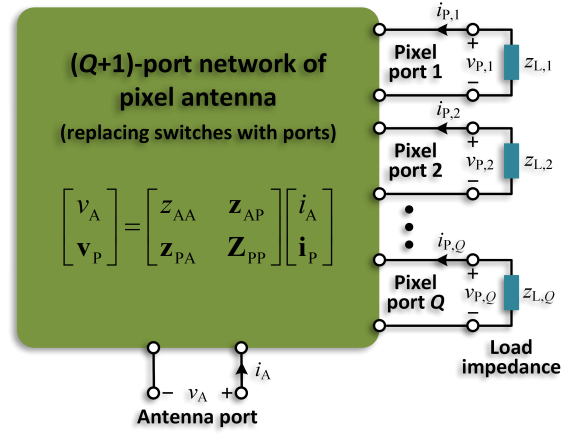
[2]It is the RF switch that has on or off states and that it is not the pixel element that has on or off states. The RF switch in off state will only make the current at the RF switch zero, but this does not mean that the surface current through the pixel element will disappear, which is because pixel elements are closely coupled with each other. In addition, control of the RF switch states can be achieved by ensuring a dc path exists through the structure by using RF chokes.

Fig. 4. System diagram of the SISO pixel antenna system.

$\mathbf{e}_\theta\left(\mathbf{b}\right),\mathbf{e}_\phi\left(\mathbf{b}\right) \in \mathbb{C}^{K\times 1}$ are θ and ϕ polarization components over K sampled spatial angles, respectively. The radiation pattern of the pixel antenna is the superposition of the radiation patterns of antenna and pixel ports weighted by currents. Thus we can express $\mathbf{e}\left(\mathbf{b}\right)$ as

$$\mathbf{e}\left(\mathbf{b}\right) = \mathbf{e}_\text{A}i_\text{A} + \sum_{q=1}^{Q} \mathbf{e}_{\text{P},q}i_{\text{P},q}\left(\mathbf{b}\right) = \mathbf{E}_\text{oc}\mathbf{i}\left(\mathbf{b}\right), \qquad (6)$$

where $\mathbf{e}_\text{A} = [\mathbf{e}_{\text{A},\theta}^T, \mathbf{e}_{\text{A},\phi}^T]^T \in \mathbb{C}^{2K\times 1}$ is the radiation pattern (with $\mathbf{e}_{\text{A},\theta}, \mathbf{e}_{\text{A},\phi} \in \mathbb{C}^{K\times 1}$ being θ and ϕ polarization components) of the antenna port excited by a unit current when all the other ports are open-circuited, $\mathbf{e}_{\text{P},q} = [\mathbf{e}_{\text{P},q,\theta}^T, \mathbf{e}_{\text{P},q,\phi}^T]^T \in \mathbb{C}^{2K\times 1}$ is the radiation pattern (with $\mathbf{e}_{\text{P},q,\theta}, \mathbf{e}_{\text{P},q,\phi} \in \mathbb{C}^{K\times 1}$ being θ and ϕ polarization components) of the qth pixel port excited by unit current when all the other ports are open-circuit, the matrix $\mathbf{E}_\text{oc} = [\mathbf{e}_\text{A},\mathbf{e}_{\text{P},1},\dots,\mathbf{e}_{\text{P},Q}] \in \mathbb{C}^{2K\times (Q+1)}$ collects the open-circuit radiation patterns of all ports and is named as open-circuit radiation pattern matrix, and $\mathbf{i}\left(\mathbf{b}\right) \in \mathbb{C}^{(Q+1)\times 1}$ collects the currents at all port, expressed as

$$\mathbf{i}\left(\mathbf{b}\right) = \begin{bmatrix} i_\text{A} \\ \mathbf{i}_\text{P}\left(\mathbf{b}\right) \end{bmatrix} = \begin{bmatrix} 1 \\ -\left(\mathbf{Z}_\text{PP} + \mathbf{Z}_\text{L}\left(\mathbf{b}\right)\right)^{-1}\mathbf{z}_\text{PA} \end{bmatrix} i_\text{A}. \quad (7)$$

The load impedance matrix $\mathbf{Z}_\text{L}\left(\mathbf{b}\right)$ can be coded by the antenna coder $\mathbf{b}$, which enables coding of the currents $\mathbf{i}\left(\mathbf{b}\right)$ and radiation pattern of the pixel antenna $\mathbf{e}\left(\mathbf{b}\right)$. Thus, given the impedance matrix $\mathbf{Z}$ and open-circuit radiation pattern matrix $\mathbf{E}_\text{oc}$, we can find the radiation pattern of pixel antenna $\mathbf{e}\left(\mathbf{b}\right)$ configured by any antenna coder by (6) and (7) with low computational complexity of $\mathcal{O}\left(Q^3 + Q^2 + Q + 2K(Q+1)\right)$. In Section V-D, we will show that this multiport circuit network model has the same accuracy as the full-wave EM simulation but requires significantly less computational time.

In total, there are 2^Q different combinations for the antenna coders and each antenna coder produces distinct radiation patterns. As a result, we can select the antenna coder $\mathbf{b}$ among a wide range of 2^Q combinations to find the optimum radiation pattern for wireless systems. In the following sections, we will introduce SISO and MIMO pixel antenna systems and show the antenna coding design for enhancing wireless systems.

III. SISO PIXEL ANTENNA SYSTEM

As a starting point, we first introduce a SISO pixel antenna system, which is the simplest form for utilizing pixel antennas, to demonstrate the beamspace channel model, the antenna coding design, and codebook design for antenna coding.

A. Beamspace Channel Model

The SISO pixel antenna system is equipped with a conventional antenna at the transmitter and a pixel antenna at the receiver, as shown in Fig. 4. To model the channel for the SISO pixel antenna system, we use the beamspace channel representation [35], [36]. Specifically, utilizing a virtual channel representation, we can represent the beamspace channel model in the angular domain, written as

$$h\left(\mathbf{b}_\text{R}\right) = \mathbf{e}_\text{R}^T\left(\mathbf{b}_\text{R}\right)\mathbf{H}_\text{V}\mathbf{e}_\text{T} \qquad (8)$$

where $\mathbf{e}_\text{T}$ is the normalized radiation pattern of the conventional antenna at the transmitter satisfying $\|\mathbf{e}_\text{T}\| = 1$, $\mathbf{e}_\text{R}\left(\mathbf{b}_\text{R}\right)$ is the normalized radiation pattern of the pixel antenna coded by antenna coder $\mathbf{b}_\text{R}$ at the receiver satisfying $\|\mathbf{e}_\text{R}\left(\mathbf{b}_\text{R}\right)\| = 1$, and $\mathbf{H}_\text{V} \in \mathbb{C}^{2K\times 2K}$ is the virtual channel matrix given by

$$\mathbf{H}_\text{V} = \begin{bmatrix} \mathbf{H}_{\text{V},\theta\theta} & \mathbf{H}_{\text{V},\theta\phi} \\ \mathbf{H}_{\text{V},\phi\theta} & \mathbf{H}_{\text{V},\phi\phi} \end{bmatrix}, \qquad (9)$$

where $\mathbf{H}_{\text{V},\theta\theta}$, $\mathbf{H}_{\text{V},\theta\phi}$, $\mathbf{H}_{\text{V},\phi\theta}$, $\mathbf{H}_{\text{V},\phi\phi} \in \mathbb{C}^{K\times K}$ are the virtual channel matrices for θ and ϕ polarizations, respectively, with each entry being the channel gain from an angle of departure (AoD) to an angle of arrival (AoA) among the K spatial angles. We consider a rich scattering environment with Rayleigh fading and assume that $[\mathbf{H}_\text{V}]_{i,j} \,\forall i,j$ are independent and identically distributed (i.i.d.) random variables following the complex Gaussian distribution $\mathcal{CN}\left(0,1\right)$.

From the beamspace channel model (8), we can see that the channel of SISO pixel antenna system $h\left(\mathbf{b}_\text{R}\right)$ can be coded by the antenna coder $\mathbf{b}_\text{R}$, which allows the antenna coding optimization to control the channel and enhance the system.

B. Antenna Coding Design

For the SISO pixel antenna system, the received signal $y \in \mathbb{C}$ can be expressed as

$$y = h\left(\mathbf{b}_\text{R}\right)x + n, \qquad (10)$$

where $x \in \mathbb{C}$ is the transmit signal and $n \in \mathbb{C}$ is additive white Gaussian noise following the complex Gaussian distribution $\mathcal{CN}\left(0,\sigma^2\right)$. Leveraging (8) and (10), the channel gain for the SISO pixel antenna system is given by

$$|h\left(\mathbf{b}_\text{R}\right)|^2 = \left|\mathbf{e}_\text{R}^T\left(\mathbf{b}_\text{R}\right)\mathbf{H}_\text{V}\mathbf{e}_\text{T}\right|^2. \qquad (11)$$

Assuming the channel state information (CSI) for the virtual channel matrix $\mathbf{H}_\text{V}$ is perfectly known as the CSI can be estimated by using methods in [37], we aim to optimize

the antenna coder for the pixel antenna $\mathbf{b}_R$ to maximize the channel gain, formulated as

$$\max_{\mathbf{e}_R, \mathbf{b}_R, \mathbf{i}_R, i_A^R} \left| \mathbf{e}_R^T (\mathbf{b}_R) \mathbf{H}_V \mathbf{e}_T \right|^2 \tag{12}$$

$$\text{s.t.} \quad \| \mathbf{e}_R (\mathbf{b}_R) \| = 1, \tag{13}$$

$$\mathbf{e}_R (\mathbf{b}_R) = \mathbf{E}_{oc} \mathbf{i}_R (\mathbf{b}_R), \tag{14}$$

$$\mathbf{i}_R (\mathbf{b}_R) = \begin{bmatrix} 1 \\ -(\mathbf{Z}_{PP} + \mathbf{Z}_L (\mathbf{b}_R))^{-1} \mathbf{z}_{PA} \end{bmatrix} i_A^R, \tag{15}$$

$$[\mathbf{b}_R]_q \in \{0, 1\}, \forall q, \tag{16}$$

where $\mathbf{i}_R (\mathbf{b}_R)$ is the currents at all ports of the pixel antenna coded by $\mathbf{b}_R$ at the receiver and i_A^R is the current at the antenna port. i_A^R is an optimization variable to ensure that the constraint (13) can be satisfied for any given $\mathbf{b}_R$.

To handle the constraint (13), we normalize the radiation pattern $\mathbf{e}_R (\mathbf{b}_R)$ and therefore equivalently transform the problem (12)-(16) as

$$\max_{\mathbf{e}_R, \mathbf{b}_R, \bar{\mathbf{i}}_R} \left| \mathbf{e}_R^T (\mathbf{b}_R) \mathbf{H}_V \mathbf{e}_T \right|^2 \tag{17}$$

$$\text{s.t.} \quad \mathbf{e}_R (\mathbf{b}_R) = \frac{\mathbf{E}_{oc} \bar{\mathbf{i}}_R (\mathbf{b}_R)}{\left\| \mathbf{E}_{oc} \bar{\mathbf{i}}_R (\mathbf{b}_R) \right\|}, \tag{18}$$

$$\bar{\mathbf{i}}_R (\mathbf{b}_R) = \begin{bmatrix} 1 \\ -(\mathbf{Z}_{PP} + \mathbf{Z}_L (\mathbf{b}_R))^{-1} \mathbf{z}_{PA} \end{bmatrix}, \tag{19}$$

$$[\mathbf{b}_R]_q \in \{0, 1\}, \forall q, \tag{20}$$

where the variable i_A^R is removed because it does not affect the normalized radiation pattern. Substituting (19) into (18), we can find the expression of $\mathbf{e}_R (\mathbf{b}_R)$ as a function of $\mathbf{b}_R$ and thus equivalently simplify the problem (17)-(20) as

$$\max_{\mathbf{b}_R} \left| \mathbf{e}_R^T (\mathbf{b}_R) \mathbf{H}_V \mathbf{e}_T \right|^2 \tag{21}$$

$$\text{s.t.} \quad [\mathbf{b}_R]_q \in \{0, 1\}, \forall q, \tag{22}$$

which is an NP-hard binary optimization problem.

Various algorithms have been proposed and utilized for pixel antenna design and optimization such as the genetic algorithm [7], mixed integer linear programming [38], N-port characteristic mode analysis [39], [40], perturbation sensitivity analysis [41], the adjoint method combined with the method of moving asymptote [42], and reinforcement learning [43]. In this work, to solve the problem (21)-(22), we use an efficient algorithm called the Successive Exhaustive Boolean Optimization (SEBO) [44], which has two steps: 1) cyclically optimizing each block of the binary variables by exhaustive search until convergence, and 2) randomly flipping bits in the converged binary solution to check if there is any other local optimum with a better objective value. The computational complexity of SEBO is $\mathcal{O}(N_e 2^J)$ where J is the block size and N_e is the number of iterations. Increasing J can enhance the optimization performance. Particularly, when $J = Q$, the SEBO becomes the exhaustive search and global optimal solution can be found. However, increasing J will exponentially increase the computational complexity. Thus, there is a trade-off between the computational complexity and optimization performance when using the SEBO to optimize antenna coding. More details on SEBO can be found in [44].

C. Codebook Design for Antenna Coding

To reduce the computational complexity, we design a codebook for antenna coding optimization. Given a codebook which is defined as a set of M different antenna coders $\mathcal{B} \triangleq \{\mathbf{b}_1, \mathbf{b}_2, \ldots, \mathbf{b}_M\}$, the channel gain is maximized by selecting the antenna coder from the codebook, formulated as

$$\mathbf{b}_R^\star = \underset{\mathbf{b}_R \in \mathcal{B}}{\arg\max} \left| \mathbf{e}_R^T (\mathbf{b}_R) \mathbf{H}_V \mathbf{e}_T \right|^2. \tag{23}$$

Given a codebook and channel realization of $\mathbf{H}_V$, we can optimize the antenna coder $\mathbf{b}_R$ by searching the codebook. However, it is important to design a good codebook to maximize ergodic channel gain, formulated as

$$\max_{\mathbf{b}_m} \quad \mathbb{E} \left[\left| \mathbf{e}_R^T (\mathbf{b}_R^\star) \mathbf{H}_V \mathbf{e}_T \right|^2 \right] \tag{24}$$

$$\text{s.t.} \quad [\mathbf{b}_m]_q \in \{0, 1\}, \forall m, q. \tag{25}$$

The codebook design problem (24) and (25) is related to the vector quantization problem [45]. To handle the ergodic channel gain in (24), we leverage the sample average approximation method [46]. Specifically, we consider a training set containing L realizations for the virtual channel matrix $\mathbf{H}_V$ which is a random matrix with each entry following i.i.d. complex Gaussian distribution, given by

$$\mathcal{H} \triangleq \left\{ \mathbf{H}_V^{[l]} \mid l = 1, \ldots, L \right\}, \tag{26}$$

where $\mathbf{H}_V^{[l]}$ denotes the lth virtual channel realization. Accordingly, we can approximate the expectation of channel gain in (24) as the sample average of channel gain, written as

$$\mathbb{E} \left[\left| \mathbf{e}_R^T (\mathbf{b}_R^\star) \mathbf{H}_V \mathbf{e}_T \right|^2 \right] \approx \frac{1}{L} \sum_{l=1}^{L} \left| \mathbf{e}_R^T (\mathbf{b}_R^\star) \mathbf{H}_V^{[l]} \mathbf{e}_T \right|^2. \tag{27}$$

Associated with each antenna coder, we can partition the training set $\mathcal{H}$ into M subsets $\mathcal{H}_1, \mathcal{H}_2, \ldots, \mathcal{H}_M$, where $\mathcal{H}_m$ is the neighborhood of the antenna coder $\mathbf{b}_m$ defined as

$$\mathcal{H}_m = \left\{ \mathbf{H}_V^{[l]} \mid \left| \mathbf{e}_R^T (\mathbf{b}_m) \mathbf{H}_V^{[l]} \mathbf{e}_T \right|^2 \right.$$
$$\left. \geq \left| \mathbf{e}_R^T (\mathbf{b}_{m'}) \mathbf{H}_V^{[l]} \mathbf{e}_T \right|^2, \forall l, \forall m' \neq m \right\}, \forall m. \tag{28}$$

Making use of (27) and (28), we can equivalently reformulate the problem (24) and (25) as

$$\max_{\mathbf{b}_m} \quad \sum_{m=1}^{M} \sum_{\mathbf{H}_V^{[l]} \in \mathcal{H}_m} \left| \mathbf{e}_R^T (\mathbf{b}_m) \mathbf{H}_V^{[l]} \mathbf{e}_T \right|^2 \tag{29}$$

$$\text{s.t.} \quad [\mathbf{b}_m]_q \in \{0, 1\}, \forall m, q. \tag{30}$$

Note that to ensure that the sample average accurately approximates the ergodic channel gain, the entries of training set should be the independent realizations of random $\mathbf{H}_V$ and the size of training set L should be large enough compared to the codebook size. Otherwise, such approximation is inaccurate and will degrade the codebook design.

We can see that the partition of training set $\mathcal{H}_m$ $\forall m$ relies on the antenna coder $\mathbf{b}_m$ $\forall m$ in the problem (29) and (30). Such coupled $\mathcal{H}_m$ and $\mathbf{b}_m$ make the problem (29) and (30)

Algorithm 1 Codebook Design for Antenna Coding

Input: $\mathcal{H}$;
Output: Codebook design $\mathcal{B}$;
1: **Initialization:** $i = 0$, $\mathbf{b}_m^{(0)}$ $\forall m$;
2: **repeat**
$\quad\quad i = i + 1$;
3: $\quad$ **Partition Optimization:**
$\quad\quad$ Update $\mathcal{H}_m^{(i)}$ $\forall m$ by (31) with $\mathbf{b}_m^{(i-1)}$;
4: $\quad$ **Antenna Coder Optimization:**
$\quad\quad$ Update $\mathbf{b}_m^{(i)}$ $\forall m$ by solving (32) with $\mathcal{H}_m^{(i)}$;
5: **until** $\sum \left\| \mathbf{b}_m^{(i)} - \mathbf{b}_m^{(i-1)} \right\| / \sum \left\| \mathbf{b}_m^{(i)} \right\| \leq \epsilon$ or $i = i_{\max}$;
6: Obtain $\mathbf{b}_m = \mathbf{b}_m^{(i)}$ $\forall m$;
7: Obtain $\mathcal{B} \triangleq \{\mathbf{b}_1, \mathbf{b}_2, \ldots, \mathbf{b}_M\}$

---

intractable. To address the problem (29) and (30), we follow the framework of the generalized Lloyd algorithm (GLA) [47] to optimize the training set partition $\mathcal{H}_m$ and antenna coder $\mathbf{b}_m$ alternatively via leveraging the nearest neighbor rule and the centroid condition. The methods are described next.

1) Partition Optimization: One necessary condition for the optimal codebook is the nearest neighbor rule. Namely, all the channel realizations which have higher channel gain with the antenna coder $\mathbf{b}_m$ than with any other antenna coders should be assigned to the partition $\mathcal{H}_m$. Therefore, at iteration i of the alternating optimization, we first optimize the partition by

$$\mathcal{H}_m^{(i)} = \left\{ \mathbf{H}_V^{[l]} \mid \left| \mathbf{e}_R^T \left(\mathbf{b}_m^{(i-1)} \right) \mathbf{H}_V^{[l]} \mathbf{e}_T \right|^2 \right.$$
$$\left. \geq \left| \mathbf{e}_R^T \left(\mathbf{b}_{m'}^{(i-1)} \right) \mathbf{H}_V^{[l]} \mathbf{e}_T \right|^2, \forall l, \forall m' \neq m \right\}, \forall m. \tag{31}$$

where $\mathbf{b}_m^{(i-1)}$ is the antenna coder optimized at iteration $i-1$.

2) Antenna Coder Optimization: The other necessary condition for the optimal codebook is the centroid condition. Namely, the optimal antenna coder $\mathbf{b}_m$ should be selected to maximize the average channel gain over the partition $\mathcal{H}_m$. Therefore, at iteration i, after the partition optimization, we then optimize the antenna coder by

$$\mathbf{b}_m^{(i)} = \operatorname*{argmax}_{[\mathbf{b}_m]_q \in \{0,1\}, \forall m, q} \sum_{\mathbf{H}_V^{[l]} \in \mathcal{H}_m^{(i)}} \left| \mathbf{e}_R^T \left(\mathbf{b}_m \right) \mathbf{H}_V^{[l]} \mathbf{e}_T \right|^2, \forall m, \tag{32}$$

which is a binary optimization problem that can be solved by the SEBO algorithm.

By alternatively optimizing the partition (31) and the antenna coder (32), the average channel gain increases over each iteration so that the codebook design converges. Algorithm 1 summarizes the overall algorithm for codebook design.

D. Performance Analysis

In order to obtain insights into the fundamental limits of pixel antennas, we derive the upper bound of the channel gain of SISO pixel antenna system as follows.

Using singular value decomposition (SVD), we can decompose the open-circuit radiation pattern matrix $\mathbf{E}_{\mathrm{oc}}$ as

$$\mathbf{E}_{\mathrm{oc}} = \mathbf{U}\mathbf{S}\mathbf{V}^H \tag{33}$$

where $R = \mathrm{rank}\left(\mathbf{E}_{\mathrm{oc}} \right)$ is the rank of matrix $\mathbf{E}_{\mathrm{oc}}$, $\mathbf{U} \in \mathbb{C}^{2K \times R}$ and $\mathbf{V} \in \mathbb{C}^{(Q+1) \times R}$ are semi-unitary matrices satisfying $\mathbf{U}^H \mathbf{U} = \mathbf{V}^H \mathbf{V} = \mathbf{I}$, and $\mathbf{S} = \mathrm{diag}\left(s_1, \ldots, s_R \right) \in \mathbb{R}^{R \times R}$ with s_i representing the ith singular value. Making use of (6) and (33), we can rewrite $\mathbf{e}_R\left(\mathbf{b}_R \right)$ as

$$\mathbf{e}_R\left(\mathbf{b}_R \right) = \mathbf{E}_{\mathrm{oc}} \mathbf{i}_R\left(\mathbf{b}_R \right) = \mathbf{U}\mathbf{S}\mathbf{V}^H \mathbf{i}_R\left(\mathbf{b}_R \right). \tag{34}$$

This shows that any possible radiation pattern generated by the pixel antenna can be decomposed into R orthogonal radiation patterns, i.e. the R columns of $\mathbf{U}$. In the beamspace domain, the number of orthogonal radiation patterns that antennas can provide is defined as effective aerial degrees-of-freedom (EADoF) [48]. Hence, the EADoF of pixel antennas is given by R. Moreover, the singular value s_i reflects the ability to radiate for the ith orthogonal radiation pattern. In other words, s_i^2 characterizes how much the power of the ith orthogonal radiation pattern is in the total radiated power. Thus, a high value of s_i^2 implies that the ith orthogonal radiation pattern is dominant in the total radiation pattern of the pixel antenna.

Accordingly, substituting (34) into (8), we can rewrite the beamspace channel of the SISO pixel antenna system as

$$h\left(\mathbf{b}_R \right) = \mathbf{i}_R^T \left(\mathbf{b}_R \right) \mathbf{V}^* \mathbf{S} \mathbf{U}^T \mathbf{H}_V \mathbf{e}_T = \mathbf{w}^H \left(\mathbf{b}_R \right) \widetilde{\mathbf{h}}, \tag{35}$$

where $\mathbf{w}\left(\mathbf{b}_R \right) \in \mathbb{C}^{R \times 1}$ is defined as

$$\mathbf{w}\left(\mathbf{b}_R \right) = \mathbf{S}\mathbf{V}^T \mathbf{i}_R^*\left(\mathbf{b}_R \right), \tag{36}$$

which satisfies $\|\mathbf{w}\left(\mathbf{b}_R \right)\| = 1$ due to the normalized radiation pattern $\|\mathbf{e}_R\left(\mathbf{b}_R \right)\| = 1$, and $\widetilde{\mathbf{h}} \in \mathbb{C}^{R \times 1}$ is defined as

$$\widetilde{\mathbf{h}} = \mathbf{U}^T \mathbf{H}_V \mathbf{e}_T, \tag{37}$$

where $[\widetilde{\mathbf{h}}]_i$ $\forall i$ are i.i.d. random variables following the complex Gaussian distribution $\mathcal{CN}\left(0, 1 \right)$ because of the R orthogonal radiation patterns collected in $\mathbf{U}$.

From (35), we can observe that the channel of SISO pixel antenna system (with a conventional antenna at the transmitter and a pixel antenna at the receiver) is equivalent to a single-input multiple-output (SIMO) channel with combining. Therefore, we can find an upper bound for the channel gain of SISO pixel antenna system using Cauchy-Schwarz inequality

$$|h\left(\mathbf{b}_R \right)|^2 = \left| \mathbf{w}^H\left(\mathbf{b}_R \right) \widetilde{\mathbf{h}} \right|^2 \leq \left\| \widetilde{\mathbf{h}} \right\|^2, \tag{38}$$

where the upper bound is achieved if and only if the maximum ratio combiner is achieved, i.e.

$$\mathbf{w}\left(\mathbf{b}_R \right) = \frac{\widetilde{\mathbf{h}}}{\left\| \widetilde{\mathbf{h}} \right\|}. \tag{39}$$

However, it should be noted that for pixel antennas there is no guarantee that an antenna coder $\mathbf{b}_R$, such that $\mathbf{w}\left(\mathbf{b}_R \right)$ satisfies (39), can be found. Therefore the upper bound for channel gain can be approached but cannot be guaranteed to be achieved.
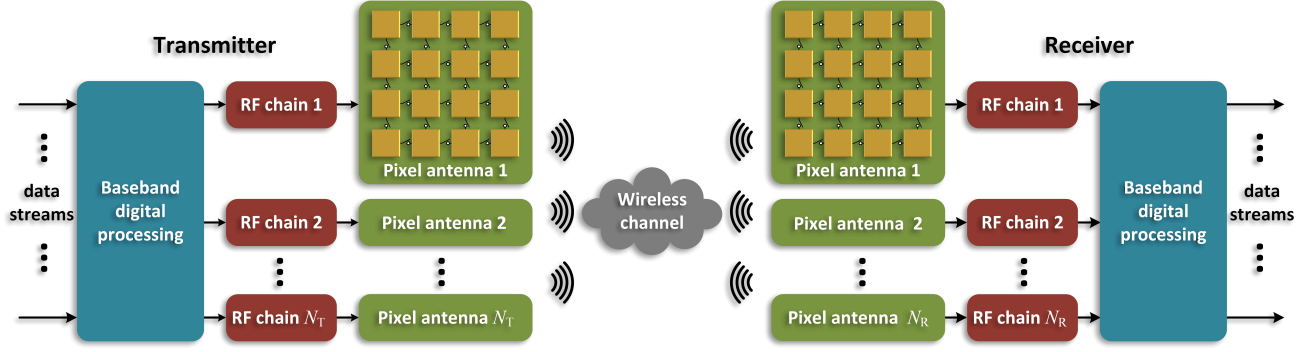
Fig. 5. System diagram of the MIMO pixel antenna system.

Accordingly, the upper bound for the average channel gain of SISO pixel antenna system is given by

$$\mathbb{E}\left[|h\left(\mathbf{b}_{\mathrm{R}}\right)|^2\right] \le \mathbb{E}\left[\left\|\widetilde{\mathbf{h}}\right\|^2\right] = R. \tag{40}$$

Therefore, this indicates that the average channel gain of the SISO pixel antenna system is upper bounded by how many orthogonal radiation patterns the pixel antenna can generate, i.e. the EADoF of pixel antennas, which is determined by the physical aperture of the pixel antenna[3]. The average channel gain in comparison with the corresponding upper bound for SISO pixel antenna system with different physical apertures will be shown in Section V.

IV. MIMO PIXEL ANTENNA SYSTEM

We introduce a MIMO pixel antenna system to demonstrate the beamspace channel model and antenna coding design for capacity maximization in this section.

A. Beamspace Channel Model

We consider a MIMO pixel antenna system. As shown in Fig. 5, the transmitter is equipped with N_{T} pixel antennas, each of which is coded by $\mathbf{b}_{\mathrm{T},n_{\mathrm{T}}} \forall n_{\mathrm{T}}$, and the receiver is equipped with N_{R} pixel antennas, each of which is coded by $\mathbf{b}_{\mathrm{R},n_{\mathrm{R}}} \forall n_{\mathrm{R}}$. We group $\mathbf{b}_{\mathrm{T},n_{\mathrm{T}}} \forall n_{\mathrm{T}}$ into a matrix $\mathbf{B}_{\mathrm{T}} = [\mathbf{b}_{\mathrm{T},1}, \ldots, \mathbf{b}_{\mathrm{T},N_{\mathrm{T}}}] \in \mathbb{R}^{Q \times N_{\mathrm{T}}}$ and $\mathbf{b}_{\mathrm{R},n_{\mathrm{R}}} \forall n_{\mathrm{R}}$ into a matrix $\mathbf{B}_{\mathrm{R}} = [\mathbf{b}_{\mathrm{R},1}, \ldots, \mathbf{b}_{\mathrm{R},N_{\mathrm{R}}}] \in \mathbb{R}^{Q \times N_{\mathrm{R}}}$. Utilizing the beamspace channel representation, the channel for MIMO pixel antenna system can be expressed as

$$\mathbf{H}\left(\mathbf{B}_{\mathrm{T}}, \mathbf{B}_{\mathrm{R}}\right) = \mathbf{E}_{\mathrm{R}}^T\left(\mathbf{B}_{\mathrm{R}}\right) \mathbf{H}_{\mathrm{V}} \mathbf{E}_{\mathrm{T}}\left(\mathbf{B}_{\mathrm{T}}\right) \tag{41}$$

where $\mathbf{E}_{\mathrm{T}}\left(\mathbf{B}_{\mathrm{T}}\right) \triangleq [\mathbf{e}_{\mathrm{T},1}\left(\mathbf{b}_{\mathrm{T},1}\right), \ldots, \mathbf{e}_{\mathrm{T},N_{\mathrm{T}}}\left(\mathbf{b}_{\mathrm{T},N_{\mathrm{T}}}\right)] \in \mathbb{C}^{2K \times N_{\mathrm{T}}}$ with $\mathbf{e}_{\mathrm{T},n_{\mathrm{T}}}\left(\mathbf{b}_{\mathrm{T},n_{\mathrm{T}}}\right)$ being the normalized radiation pattern of the n_{T}th transmit pixel antenna satisfying $\|\mathbf{e}_{\mathrm{T},n_{\mathrm{T}}}\left(\mathbf{b}_{\mathrm{T},n_{\mathrm{T}}}\right)\| = 1$, $\mathbf{E}_{\mathrm{R}}\left(\mathbf{B}_{\mathrm{R}}\right) \triangleq [\mathbf{e}_{\mathrm{R},1}\left(\mathbf{b}_{\mathrm{R},1}\right), \ldots, \mathbf{e}_{\mathrm{R},N_{\mathrm{R}}}\left(\mathbf{b}_{\mathrm{R},N_{\mathrm{R}}}\right)] \in \mathbb{C}^{2K \times N_{\mathrm{R}}}$ with $\mathbf{e}_{\mathrm{R},n_{\mathrm{R}}}\left(\mathbf{b}_{\mathrm{R},n_{\mathrm{R}}}\right)$ being the normalized radiation pattern of the n_{R}th receive pixel antenna satisfying $\|\mathbf{e}_{\mathrm{R},n_{\mathrm{R}}}\left(\mathbf{b}_{\mathrm{R},n_{\mathrm{R}}}\right)\| = 1$, and $\mathbf{H}_{\mathrm{V}} \in \mathbb{C}^{2K \times 2K}$ is the virtual channel matrix given by (9). Similarly, from the beamspace channel model (41), we can see that the channel of MIMO pixel antenna system $\mathbf{H}\left(\mathbf{B}_{\mathrm{T}}, \mathbf{B}_{\mathrm{R}}\right)$ can be coded by the transmit and receive antenna coders $\mathbf{B}_{\mathrm{T}}$ and $\mathbf{B}_{\mathrm{R}}$, which allows antenna coding optimization to enhance the MIMO system.

[3]It is difficult to write the relationship between EADoF and aperture in closed form as $\mathbf{E}_{\mathrm{oc}}$ is obtained by simulating the pixel antenna by EM solver.

B. Channel Capacity

For the MIMO pixel antenna system, the received signal $\mathbf{y} \in \mathbb{C}^{N_{\mathrm{R}} \times 1}$ can be expressed as

$$\mathbf{y} = \mathbf{H}\left(\mathbf{B}_{\mathrm{T}}, \mathbf{B}_{\mathrm{R}}\right) \mathbf{x} + \mathbf{n}, \tag{42}$$

where $\mathbf{x} \in \mathbb{C}^{N_{\mathrm{T}} \times 1}$ is the transmit signal with covariance matrix given by $\mathbf{X} = \mathbb{E}\left[\mathbf{x}\mathbf{x}^H\right]$ and $\mathbf{n} \in \mathbb{C}^{N_{\mathrm{R}} \times 1}$ is the additive white Gaussian noise following the complex Gaussian distribution $\mathcal{CN}\left(\mathbf{0}, \sigma^2 \mathbf{I}\right)$. Accordingly, the channel capacity for the MIMO pixel antenna system is given by

$$C\left(\mathbf{X}, \mathbf{B}_{\mathrm{T}}, \mathbf{B}_{\mathrm{R}}\right) = \log_2\left|\mathbf{I} + \frac{1}{\sigma^2}\mathbf{H}\left(\mathbf{B}_{\mathrm{T}}, \mathbf{B}_{\mathrm{R}}\right)\mathbf{X}\mathbf{H}^H\left(\mathbf{B}_{\mathrm{T}}, \mathbf{B}_{\mathrm{R}}\right)\right|. \tag{43}$$

Assuming the CSI for the virtual channel matrix $\mathbf{H}_{\mathrm{V}}$ is perfectly known, we aim to jointly optimize the transmit signal covariance matrix $\mathbf{X}$ and the transmit and receive antenna coders $\mathbf{B}_{\mathrm{T}}$ and $\mathbf{B}_{\mathrm{R}}$ to maximize the channel capacity for the MIMO pixel antenna system, which can be formulated as

$$\max_{\mathbf{X}, \mathbf{B}_{\mathrm{T}}, \mathbf{B}_{\mathrm{R}}} \log_2\left|\mathbf{I} + \frac{1}{\sigma^2}\mathbf{H}\left(\mathbf{B}_{\mathrm{T}}, \mathbf{B}_{\mathrm{R}}\right)\mathbf{X}\mathbf{H}^H\left(\mathbf{B}_{\mathrm{T}}, \mathbf{B}_{\mathrm{R}}\right)\right| \tag{44}$$

$$\text{s.t.} \quad \mathrm{Tr}\left(\mathbf{X}\right) \le P, \tag{45}$$

$$[\mathbf{B}_{\mathrm{T}}]_{i,j} \in \{0, 1\}, \forall i, j, \tag{46}$$

$$[\mathbf{B}_{\mathrm{R}}]_{i,j} \in \{0, 1\}, \forall i, j, \tag{47}$$

where P denotes the maximum transmit power.

C. Antenna Coding Design

To solve the capacity maximization problem (44)-(47), in the following, we consider two cases of the transmit signal covariance matrix.

1) Antenna Coding Design with Uniform Power Allocation: We first consider when the uniform power allocation is utilized in the MIMO pixel antenna system, i.e. $\mathbf{X} = \frac{P}{N_{\mathrm{T}}}\mathbf{I}$. In this case, we only need to optimize the transmit and receive antenna coders $\mathbf{B}_{\mathrm{T}}$ and $\mathbf{B}_{\mathrm{R}}$ for capacity maximization, formulated as

$$\max_{\mathbf{B}_{\mathrm{T}}, \mathbf{B}_{\mathrm{R}}} \log_2\left|\mathbf{I} + \frac{P}{\sigma^2 N_{\mathrm{T}}}\mathbf{H}\left(\mathbf{B}_{\mathrm{T}}, \mathbf{B}_{\mathrm{R}}\right)\mathbf{H}^H\left(\mathbf{B}_{\mathrm{T}}, \mathbf{B}_{\mathrm{R}}\right)\right| \tag{48}$$

$$\text{s.t.} \quad [\mathbf{B}_{\mathrm{T}}]_{i,j} \in \{0, 1\}, \forall i, j, \tag{49}$$

$$[\mathbf{B}_{\mathrm{R}}]_{i,j} \in \{0, 1\}, \forall i, j, \tag{50}$$

which is an NP-hard binary optimization problem. Similar to the channel gain maximization in the SISO pixel antenna, we use the SEBO algorithm to solve the problem (48)-(50).

2) Joint Antenna Coding and Waterfilling Design: We next consider joint antenna coding and transmit signal covariance matrix design for capacity maximization in the MIMO pixel antenna system. For the channel matrix $\mathbf{H}(\mathbf{B}_{\mathrm{T}}, \mathbf{B}_{\mathrm{R}})$ with any given transmit and receive antenna coders $\mathbf{B}_{\mathrm{T}}$ and $\mathbf{B}_{\mathrm{R}}$, it is well known that the transmit signal covariance matrix design based on waterfilling power allocation provides the maximum channel capacity [49], i.e.

$$\sum_{i=1}^{N_{\min}} \log_2 \left(1 + \frac{P_i^\star (\mathbf{B}_{\mathrm{T}}, \mathbf{B}_{\mathrm{R}}) \lambda_i (\mathbf{B}_{\mathrm{T}}, \mathbf{B}_{\mathrm{R}})}{\sigma^2} \right), \quad (51)$$

where $N_{\min} = \min(N_{\mathrm{T}}, N_{\mathrm{R}})$, $\lambda_i (\mathbf{B}_{\mathrm{T}}, \mathbf{B}_{\mathrm{R}})$ is the ith eigenvalue of the matrix $\mathbf{H}(\mathbf{B}_{\mathrm{T}}, \mathbf{B}_{\mathrm{R}}) \mathbf{H}^H (\mathbf{B}_{\mathrm{T}}, \mathbf{B}_{\mathrm{R}})$, and $P_i^\star (\mathbf{B}_{\mathrm{T}}, \mathbf{B}_{\mathrm{R}})$ represents the waterfilling power allocation expressed as

$$P_i^\star (\mathbf{B}_{\mathrm{T}}, \mathbf{B}_{\mathrm{R}}) = \left(\mu - \frac{\sigma^2}{\lambda_i (\mathbf{B}_{\mathrm{T}}, \mathbf{B}_{\mathrm{R}})} \right)^+, \quad (52)$$

with μ chosen to satisfy the total transmit power constraint

$$\sum_{i=1}^{N_{\min}} P_i^\star (\mathbf{B}_{\mathrm{T}}, \mathbf{B}_{\mathrm{R}}) = P. \quad (53)$$

As a result, the channel capacity with waterfilling power allocation is also a function of $\mathbf{B}_{\mathrm{T}}$ and $\mathbf{B}_{\mathrm{R}}$, so that the antenna coding design can be formulated as

$$\max_{\mathbf{B}_{\mathrm{T}}, \mathbf{B}_{\mathrm{R}}} \sum_{i=1}^{N_{\min}} \log_2 \left(1 + \frac{P_i^\star (\mathbf{B}_{\mathrm{T}}, \mathbf{B}_{\mathrm{R}}) \lambda_i (\mathbf{B}_{\mathrm{T}}, \mathbf{B}_{\mathrm{R}})}{\sigma^2} \right) \quad (54)$$

$$\text{s.t.} \quad [\mathbf{B}_{\mathrm{T}}]_{i,j} \in \{0, 1\}, \ \forall i, j, \quad (55)$$

$$[\mathbf{B}_{\mathrm{R}}]_{i,j} \in \{0, 1\}, \ \forall i, j, \quad (56)$$

which is an NP-hard binary optimization problem. Similarly, we use the SEBO algorithm to solve the problem (54)-(56).

D. Antenna Coding Design with Codebook

To reduce computational complexity, we use the codebook proposed in Section III-C to facilitate antenna coding design in the MIMO pixel antenna system. Specifically, given the codebook $\mathcal{B} \triangleq \{\mathbf{b}_1, \mathbf{b}_2, \ldots, \mathbf{b}_M\}$, we select the antenna coder for each transmit and receive pixel antenna from the codebook, i.e. $\mathbf{b}_{\mathrm{T}, n_{\mathrm{T}}}, \mathbf{b}_{\mathrm{R}, n_{\mathrm{R}}} \in \mathcal{B} \ \forall n_{\mathrm{T}}, n_{\mathrm{R}}$, to maximize the channel capacity of MIMO pixel antenna system. For the uniform power allocation case, we formulate the channel capacity maximization as

$$\max_{\mathbf{B}_{\mathrm{T}}, \mathbf{B}_{\mathrm{R}}} \log_2 \left| \mathbf{I} + \frac{P}{\sigma^2 N_{\mathrm{T}}} \mathbf{H}(\mathbf{B}_{\mathrm{T}}, \mathbf{B}_{\mathrm{R}}) \mathbf{H}^H (\mathbf{B}_{\mathrm{T}}, \mathbf{B}_{\mathrm{R}}) \right| \quad (57)$$

$$\text{s.t.} \quad [\mathbf{B}_{\mathrm{T}}]_{:,n_{\mathrm{T}}} \in \mathcal{B}, \ \forall n_{\mathrm{T}}, \quad (58)$$

$$[\mathbf{B}_{\mathrm{R}}]_{:,n_{\mathrm{R}}} \in \mathcal{B}, \ \forall n_{\mathrm{R}}. \quad (59)$$

For the waterfilling power allocation case, we formulate the channel capacity maximization as

$$\max_{\mathbf{B}_{\mathrm{T}}, \mathbf{B}_{\mathrm{R}}} \sum_{i=1}^{N_{\min}} \log_2 \left(1 + \frac{P_i^\star (\mathbf{B}_{\mathrm{T}}, \mathbf{B}_{\mathrm{R}}) \lambda_i (\mathbf{B}_{\mathrm{T}}, \mathbf{B}_{\mathrm{R}})}{\sigma^2} \right) \quad (60)$$

$$\text{s.t.} \quad [\mathbf{B}_{\mathrm{T}}]_{:,n_{\mathrm{T}}} \in \mathcal{B}, \ \forall n_{\mathrm{T}}, \quad (61)$$

$$[\mathbf{B}_{\mathrm{R}}]_{:,n_{\mathrm{R}}} \in \mathcal{B}, \ \forall n_{\mathrm{R}}. \quad (62)$$

Both the problem (57)-(59) and problem (60)-(62) can be solved by successively searching the codebook for each transmit and receive pixel antenna.

V. PERFORMANCE EVALUATION

We evaluate the performance of SISO pixel antenna system and MIMO pixel antenna system with the proposed antenna coding design in this section.

A. Simulation Setup and Pixel Antenna Design

We consider a propagation environment with rich scattering, which has a 2-D uniform power angular spectrum[4], i.e. uniform over the azimuth angle on the XOY plane, with equally likely polarization. We set the angular resolution as $\Delta\phi = 5°$ and thus we have $K = 72$ sampled angles. For the SISO pixel antenna system, we assume that the transmit antenna is fixed with an ideal isotropic radiation pattern and the receive antenna uses a pixel antenna. For the MIMO pixel antenna system, both transmit and receive antennas use pixel antennas.

We consider two examples of pixel antennas operating at 2.4 GHz where the wavelength is $\lambda = 125$ mm. The two pixel antennas are designed based on discretizing the radiating patch surface of conventional microstrip patch antennas[5] into a grid of pixels, but having different physical apertures, $0.25\lambda \times 0.25\lambda$ and $0.5\lambda \times 0.5\lambda$. The geometry and dimension for the two pixel antennas are illustrated in Fig. 6 and summarized in Table I. For both pixel antennas, there are in total 40 ports, including 1 antenna port and $Q = 39$ pixel ports, and 5×5 pixels with pixel size being 5mm $\times$ 5mm and 11mm $\times$ 11mm, respectively. The pixelized patch and ground plane are printed on the Rogers 4003C substrate, where the thickness is 1.524 mm, the permittivity is 3.55, and the loss tangent is 0.0027. We use CST studio suite, a full-wave EM solver, to simulate the $(Q+1)$-port circuit network of pixel antennas to achieve the impedance matrix $\mathbf{Z} \in \mathbb{C}^{(Q+1) \times (Q+1)}$ as well as the open-circuit radiation pattern matrix $\mathbf{E}_{\mathrm{oc}} \in \mathbb{C}^{2K \times (Q+1)}$.

The singular values $s_i \ \forall i$ (sorted in descending order) of the open-circuit radiation pattern matrix $\mathbf{E}_{\mathrm{oc}}$ for pixel antennas with different physical apertures are shown in Fig. 7. From Fig. 7, we can observe that the majority of the singular values are almost zero. For example, more than half of the singular values are smaller than 0.1. Recall that the singular value s_i reflects the ability to radiate for the ith orthogonal radiation pattern,

---

[4]Herein we consider 2-D uniform power angular spectrum for illustration. It should be noted that other power angular spectrum also applies.

[5]Herein we consider the pixelated microstrip patch antenna for illustration. However, it should be noted that pixel antenna is general and can be designed based on discretizing the continuous radiating surface of different types of antennas such as monopole antenna, not restricted to microstrip patch antenna.
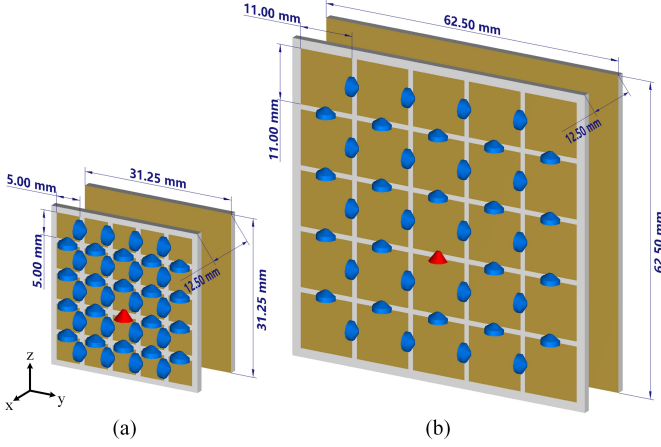
Fig. 6. Pixel antennas with different physical apertures (a) $0.25\lambda \times 0.25\lambda$ and (b) $0.5\lambda \times 0.5\lambda$. Red arrows represent the antenna ports and blue arrows represent the pixel ports.

TABLE I
GEOMETRY AND DIMENSIONS FOR PIXEL ANTENNAS

Physical aperture	$0.25\lambda \times 0.25\lambda$	$0.5\lambda \times 0.5\lambda$
Size of ground	31.25mm×31.25mm	62.5mm×62.5mm
Size of patch	29mm×29mm	59mm×59mm
Number of pixels	5×5	5×5
Size of pixel	5mm×5mm	11mm×11mm
Gap between pixels	1mm	1mm
Patch and ground spacing	12.5mm	12.5mm

i.e. s_i^2 characterizes how much the power of the ith orthogonal radiation pattern is in the total radiated power. Thus, a small value of s_i^2 implies that the ith orthogonal radiation pattern makes negligible contribution to the total radiation pattern of the pixel antennas. As a result, to identify the EADoF of the pixel antennas $R = \text{rank}(\mathbf{E}_{\text{oc}})$, i.e. how many orthogonal radiation patterns the pixel antennas can generate, we consider the cumulative distribution function of s_i^2, defined as

$$F_i = \frac{\sum_{j=1}^{i} s_j^2}{\sum_{j=1}^{Q+1} s_j^2}, \quad (63)$$

which characterizes how much power the first i orthogonal radiation patterns contribute to the total radiated power. The cumulative distribution function of s_i^2 for pixel antennas with different physical apertures are also shown in Fig. 7. We can see that the cumulative distribution function increases with the singular value index and approaches unity after a certain index. Based on this, we select the EADoF of pixel antennas as

$$R = \underset{F_i \geq T}{\text{argmin}} \, i, \quad (64)$$

which implies that the contribution of R orthogonal radiation patterns to the total radiated power is more than the threshold T. In this work, we set the threshold T as 0.998, so that the EADoF of the pixel antennas with the physical apertures $0.25\lambda \times 0.25\lambda$ and $0.5\lambda \times 0.5\lambda$ are 5 and 7, respectively. This shows that the EADoF of pixel antennas increases with the physical aperture. Moreover, recall that the upper bound for the average channel gain of SISO pixel antenna system is given
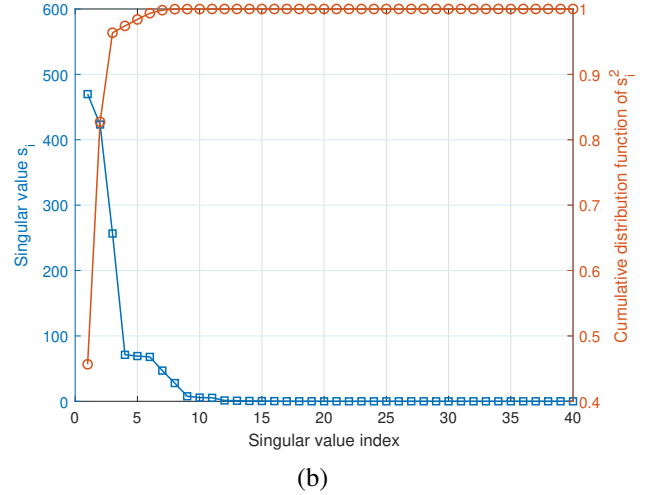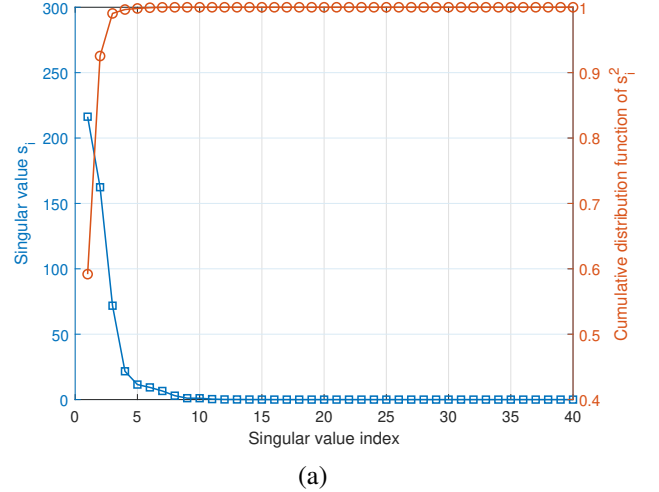

Fig. 7. Singular values s_i $\forall i$ of open-circuit radiation pattern matrix $\mathbf{E}_{\text{oc}}$ and cumulative distribution function of s_i^2 for pixel antennas with different physical apertures (a) $0.25\lambda \times 0.25\lambda$ and (b) $0.5\lambda \times 0.5\lambda$.

by the EADoF of pixel antennas. The average channel gain of SISO pixel antenna system in comparison with its upper bound will be demonstrated in the following subsection.

B. SISO Pixel Antenna System Performance

We first evaluate the performance of SISO pixel antenna system. Utilizing Monte Carlo method, we generate multiple realizations for the virtual channel matrix $\mathbf{H}_{\text{V}}$ and for each realization, we use the SEBO algorithm [44], with block size of $J = 10$ (which achieves a good optimization performance with an acceptable complexity), to solve the problem (21)-(22) so as to maximize the channel gain $|h(\mathbf{b}_{\text{R}})|^2$ with perfect CSI. In addition, we also maximize the channel gain with the codebook design for antenna coding introduced in Section III-C. The number of virtual channel realizations in the training set is $L = 15000$. The antenna coders in the codebook design with size[6] of 2, 4, and 8 are listed in Table II. The number of

---
[6]Due to limited space, it would be messy to show the antenna coders in the codebook with size larger than 8, so we omit them.

TABLE II
ANTENNA CODERS IN THE CODEBOOK WITH SIZE OF 2, 4, 8

	Physical aperture $0.25\lambda \times 0.25\lambda$	Physical aperture $0.5\lambda \times 0.5\lambda$
Codebook size = 2	0001101000000111011010110000011010011011 1010101111101101110100010011111101010101	0100001100101101011010110010100110001000 1000101010100101101100111001100000011011
Codebook size = 4	1010010111000101111100100001101100010000 1101111011110010100101101101011000101010110 1101000001000100011011111000001101111110 0101100010010001011110110101011111101110	0010101100011001011011001001000000101010 1110000111111010100000010001010000100111 1001011110010010010100100010001010001101110 1001010000100010010000100001011111100101
Codebook size = 8	0000001111100100010110111101001011101101 0001110000110110111110001101110100001011 0100111010110101100101011101110010001 0010111000000100011101101001011010101100 0101110101110001101111101111111101010 0001001010101000011011010001000010101001 0010100111110001101011110110110000000 1000010100100000111100011001000100101111110	1111101000000100010111111101001101110000 0000011010001001101010101011001011000011 1111110001110001000110010000011000010111 0100011010101011101010000100001001000000 1001001000100000000101100000101011100001111 0101111101000111000011111100100000010011 0001010011111111010101011101001111100011 1100000110110110001000010101010100000010011

(a)

(b)

Fig. 8. Average channel gain of the SISO pixel antenna system with physical apertures (a) $0.25\lambda \times 0.25\lambda$ and (b) $0.5\lambda \times 0.5\lambda$, optimized with perfect CSI and with codebook.

realizations in Monte Carlo method is 100, which is enough to obtain an accurate average performance. The average channel gain of the SISO pixel antenna system optimized with perfect CSI and with the codebook is shown in Fig. 8. The two pixel antennas with different physical apertures $0.25\lambda \times 0.25\lambda$ and $0.5\lambda \times 0.5\lambda$ are considered and the conventional SISO system is also compared as the benchmark. From Fig. 8, we can make three observations.

Firstly, compared with the conventional SISO system which has a unit average channel gain from the complex Gaussian distribution $\mathcal{CN}(0,1)$, the SISO pixel antenna system can significantly enhance the channel gain, demonstrating the benefits of pixel antennas. Specifically, the average channel gain with physical apertures $0.25\lambda \times 0.25\lambda$ and $0.5\lambda \times 0.5\lambda$ optimized with the perfect CSI are 4 and 5.4, respectively. The channel gain enhanced by SISO pixel antenna system can be explained by noting that the pixel antenna can flexibly adjust its configuration so that its radiation pattern can adapt to the virtual channel matrix to coherently add the multiple paths in the propagation environment.

Secondly, the average channel gain of SISO pixel antenna system optimized with the codebook increases with the codebook size. This is because increasing the codebook size can generate more antenna coders, so that the pixel antenna becomes more flexible and provides more diverse radiation patterns to enhance the channel. When the codebook size is large enough, the average channel gain optimized with the codebook provides performance similar to that optimized with perfect CSI. However the computational complexity for optimization can be significantly reduced. Particularly, even when the codebook size is only 2, utilizing the codebook design can still enhance the average channel gain by around 50% for different physical apertures. Therefore, this demonstrates the benefit of codebook design for pixel antennas.

Thirdly, for the SISO pixel antenna system, increasing the physical aperture is beneficial to enhance channel gain. For example, when optimized with perfect CSI, the channel gain with physical aperture $0.5\lambda \times 0.5\lambda$ is 35% higher than that with $0.25\lambda \times 0.25\lambda$. This is because pixel antennas with larger physical aperture can provide more orthogonal radiation patterns, i.e. larger EADoF. Specifically, the EADoF for the pixel antenna with physical aperture $0.25\lambda \times 0.25\lambda$ is 5 while
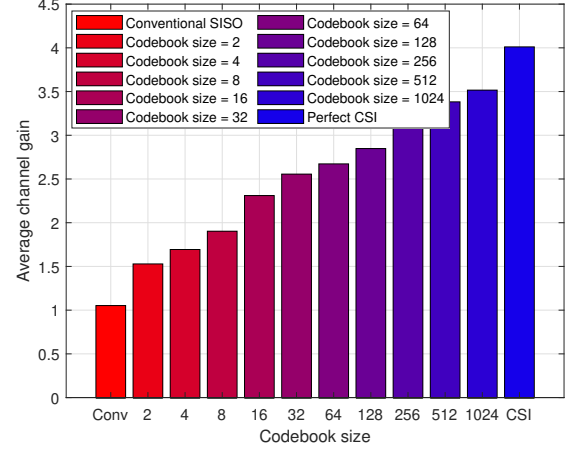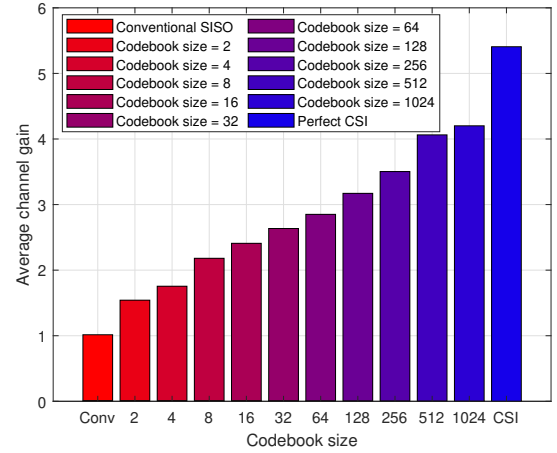
the EADoF with $0.5\lambda \times 0.5\lambda$ is 7. Therefore, pixel antennas with larger physical aperture achieve a higher upper bound for the average channel gain (40), resulting in a higher average channel gain. Moreover, it is worth noting that the upper bound of the average channel gain of SISO pixel antenna system (40) is generally hard to achieve. For example, for the physical aperture $0.25\lambda \times 0.25\lambda$, the average channel gain optimized with perfect CSI is 4 while the upper bound is 5. This is because it is not guaranteed to find the antenna coder $\mathbf{b}_R$ such that the pixel antenna current $\mathbf{i}_R(\mathbf{b}_R)$ and the $\mathbf{w}(\mathbf{b}_R)$ given by (36) satisfy the condition of maximum ratio combiner (39).

Overall, we have shown that using pixel antennas is beneficial to enhance the channel gain of SISO system.

C. MIMO Pixel Antenna System Performance

We next evaluate the performance of MIMO pixel antenna systems. Similarly, we utilize the Monte Carlo method to generate multiple realizations for the virtual channel matrix $\mathbf{H}_V$. For each realization, we optimize the antenna coding design with uniform power allocation by solving the problem
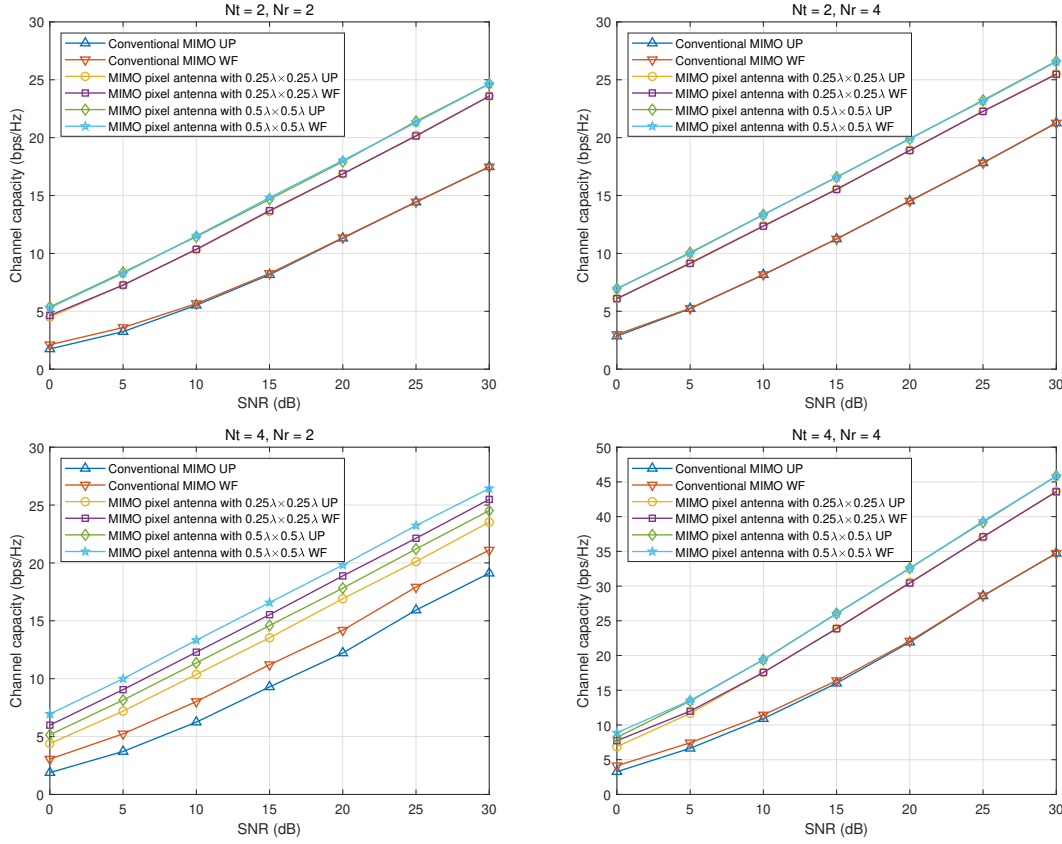
Fig. 9. Channel capacity of the conventional MIMO system and the MIMO pixel antenna system with the uniform power allocation (UP) and waterfilling (WF) optimized with perfect CSI.

(48)-(50) and also jointly optimize the antenna coding and waterfilling design by solving the problem (54)-(56), for maximizing the channel capacity of MIMO pixel antenna system with perfect CSI. The SEBO algorithm [44], with block size $J = 10$, is utilized to solve the two problems. The channel capacity of the MIMO pixel antenna system with uniform power allocation (UP) and waterfilling (WF) optimized with perfect CSI is shown in Fig. 9. The channel capacity is averaged over multiple channel realizations. The two pixel antennas with different physical apertures $0.25\lambda \times 0.25\lambda$ and $0.5\lambda \times 0.5\lambda$ are considered and the conventional MIMO system with UP and WF are compared. Different numbers of transmit and receive antennas N_T and N_R are also considered for the MIMO pixel antenna system and conventional MIMO system. From Fig. 9, we can make four observations.

Firstly, in comparison with the conventional MIMO system, the MIMO pixel antenna system can effectively enhance channel capacity, demonstrating the benefits of pixel antennas. For example, in the case of $N_T = 2$ and $N_R = 2$, the channel capacity with UP at low SNR of 0 dB for the conventional MIMO system and the MIMO pixel antenna system with physical apertures $0.25\lambda \times 0.25\lambda$ and $0.5\lambda \times 0.5\lambda$ is 1.75, 4.50, and 5.38 bps/Hz, respectively, which implies that the capacity for MIMO pixel antenna systems are 2.6 and 3.1 times higher than that for the conventional MIMO system. On the other hand, in the same case but at high SNR of 30 dB, the channel capacity with UP for the conventional MIMO system

and the MIMO pixel antenna system with physical apertures $0.25\lambda \times 0.25\lambda$ and $0.5\lambda \times 0.5\lambda$ are 17.48, 23.58 and 24.65 bps/Hz, respectively, which means that using pixel antenna can enhance the capacity by 35% and 41%. The channel capacity enhanced by MIMO pixel antenna system occurs because the multiple pixel antennas at the transmitter and receivers can flexibly adjust their radiation patterns to adapt to the virtual channel matrix $\mathbf{H}_V$ so that the multiple paths with different AoA and AoD in the propagation environment can be coherently added to enhance the channel $\mathbf{H}(\mathbf{B}_T, \mathbf{B}_R)$ in (41) as well as the capacity.

Secondly, increasing the physical aperture is beneficial to enhance the channel capacity of MIMO pixel antenna system. For example, at low SNR of 0 dB, the channel capacity with UP for MIMO pixel antenna system with physical apertures $0.5\lambda \times 0.5\lambda$ is 20% higher than that with $0.25\lambda \times 0.25\lambda$. This is because pixel antennas with larger physical aperture provide larger EADoF which increases the channel gain between each pair of transmit and receive pixel antennas and therefore leads to higher channel capacity.

Thirdly, for MIMO pixel antenna system, increasing the number of transmit antennas and receive antennas is beneficial to improve the channel capacity. For example, with the same physical aperture, the channel capacity at high SNR of 30 dB for the 4×4 MIMO pixel antenna system is nearly twice that for the 2×2 MIMO pixel antenna system, which is consistent with the conventional MIMO system. That is to say, utilizing
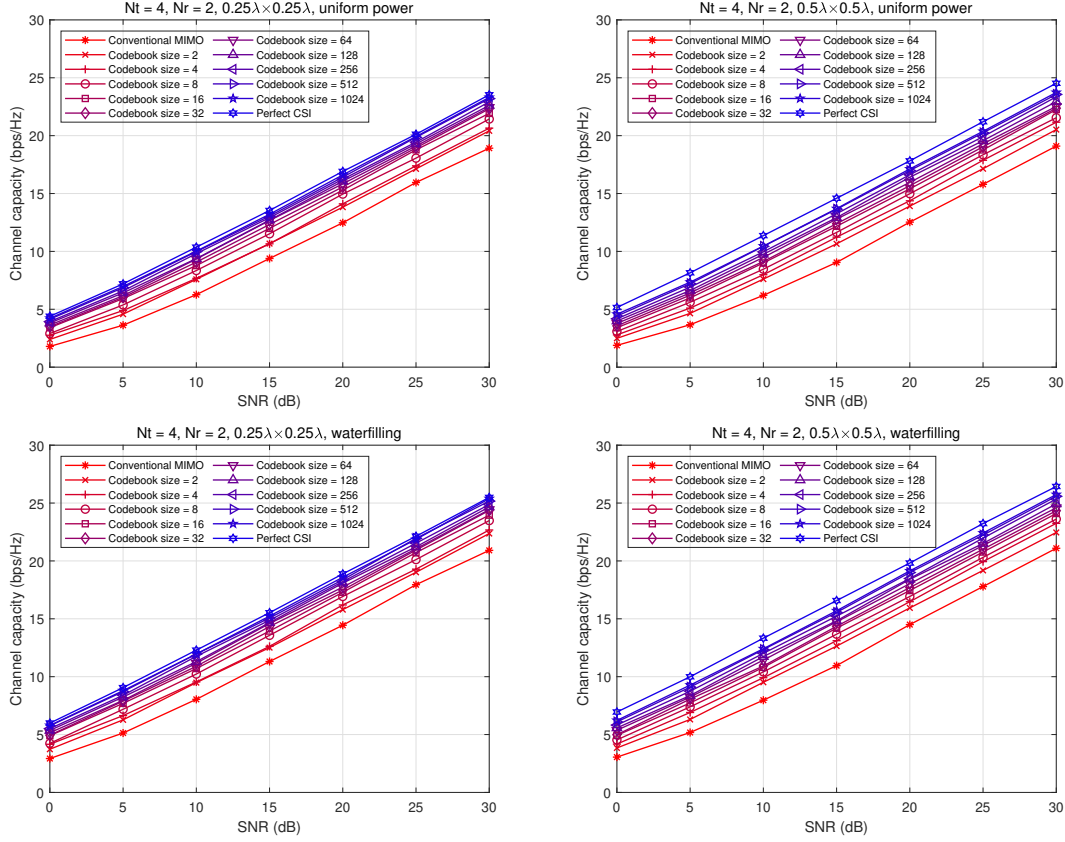
Fig. 10. Channel capacity of the MIMO pixel antenna system optimized with codebook.

pixel antennas to construct MIMO systems will not affect the multiplexing gain of MIMO system. Moreover, it will bring extra channel gain on top of the multiplexing gain.

Fourthly, the joint antenna coding and waterfilling design achieves higher channel capacity than antenna coding design with uniform power allocation, especially when there are more transmit antennas than receive antennas. For example, for the 4×2 MIMO pixel antenna system with physical aperture $0.25\lambda \times 0.25\lambda$, the channel capacity with UP and WF is 4.39 and 5.99 bps/Hz at low SNR of 0 dB, respectively. This implies that joint antenna coding and waterfilling design can increase the capacity by 36%. Thus, this shows that pixel antennas can synergize with waterfilling design to enhance channel capacity in MIMO systems.

We also use the codebook to optimize the antenna coding design with uniform power allocation and waterfilling to maximize the channel capacity of MIMO pixel antenna system. Specifically, we solve the problem (57)-(59) and problem (60)-(62) by successively searching the codebook for each transmit and receive pixel antenna. The channel capacity of the MIMO pixel antenna system with UP and WF optimized with the codebook is shown in Fig. 10. The channel capacity is averaged over channel realizations and different physical apertures are considered (we only show the 4×2 case for brevity). From Fig. 10, we can make two observations.

Firstly, the channel capacity of MIMO pixel antenna system optimized with the codebook increases with the physical

aperture. Joint antenna coding and waterfilling design achieves higher channel capacity than antenna coding design with uniform power allocation. These are consistent with the case optimized with CSI.

Secondly, the channel capacity of MIMO pixel antenna system optimized with the codebook increases with the codebook size, which is because increasing the codebook size gives the pixel antenna more diverse radiation patterns to enhance the channel. When the codebook size is large enough, the capacity optimized with codebook is similar to that optimized with perfect CSI but the computational complexity can be reduced. Even when the codebook size is only 2, using the codebook design is still beneficial. For example, the capacity with UP for the 4×2 MIMO pixel antenna system at low SNR of 0 dB is 30% higher than that for conventional MIMO system when codebook size is 2. Thus, this shows the benefit and effectiveness of codebook for MIMO pixel antenna system.

Overall, we have shown that using pixel antennas is beneficial to enhance the channel capacity of MIMO system.

D. Evaluation of Multiport Circuit Network Model

To validate the accuracy of the multiport circuit network model, we compare it with the full-wave EM simulation using CST studio suite. Specifically, in CST studio suite, we simulate the pixel antenna with physical aperture $0.5\lambda \times 0.5\lambda$ configured by different antenna coders in the codebook (with codebook size of 4). The radiation patterns of the pixel antenna, obtained

by the EM simulation and the multiport circuit network model (6) and (7), are shown in Fig. 11. We can find that the EM simulated radiation patterns are almost same as those computed by the multiport circuit network model for different antenna coders, showing the accuracy of the proposed model. In addition, the radiation patterns for different antenna coders are diverse, covering different angle ranges, which is consistent with the fact that the codebook is designed to maximize the ergodic channel gain in a multipath propagation environment with 2-D uniform power angular spectrum.

More importantly, under the same accuracy, the multiport circuit network model is significantly more computationally efficient. We measure the computational time to calculate the radiation pattern using the EM simulation (CST studio suite) and the proposed multiport circuit network model respectively, in a laptop (with AMD Ryzen 9 7940HX CPU and 16 GB memory). The average computational time for the EM simulation and the multiport circuit network model, denoted as T_{EM} and T_{circuit}, is measured around 56.59s and 0.000535s, respectively, which shows that the proposed model is around 10^5 time faster than the EM simulation.

Note that we only need one EM simulation to obtain $\mathbf{Z}$ and $\mathbf{E}_{\text{oc}}$ for the multiport circuit network model. The computational time to simulate $\mathbf{Z}$ and $\mathbf{E}_{\text{oc}}$ for a realistic pixel antenna is acceptable as the number of pixels is generally not too large with the size of pixel around 0.1-0.2λ, which is small enough to achieve high reconfigurability[7]. In this work, the computational time of the EM simulation to obtain $\mathbf{Z}$ and $\mathbf{E}_{\text{oc}}$, denoted as T_0, is measured around 12 minutes[8] by the same laptop above. In spite of such time, the EM simulation can be done offline and once $\mathbf{Z}$ and $\mathbf{E}_{\text{oc}}$ are known the radiation pattern can be calculated accurately and efficiently for real-time antenna coding optimization.

Last but not least, we completely compare the computational time for the whole process to optimize the antenna coder using the proposed multiport circuit network model and the EM simulation in the following two cases.

First, when using SEBO to optimize the antenna coder, i.e. solving the problem (21)-(22), the total number of calculations of radiation pattern is $N_e 2^J$, so the total computational time for the proposed multiport circuit network model is

$$T_{\text{total,circuit}} = T_0 + N_e 2^J T_{\text{circuit}}, \quad (65)$$

while the total computational time using EM simulation is

$$T_{\text{total,EM}} = N_e 2^J T_{\text{EM}}. \quad (66)$$

If considering $N_e = 4$ (the least number to optimize all the Q switches), we have $T_{\text{total,circuit}} = 722$ s and $T_{\text{total,EM}} = 231792$ s.

<hr>

[7]Further reducing the size of pixel can bring marginal gain but at the expense of high circuit complexity to control massive switches. Thus, it is unnecessary to have a very large number of pixels with very small pixels.

[8]When using CST studio suite to simulate the multiport circuit network of pixel antenna, the $(Q+1) \times (Q+1)$ impedance matrix $\mathbf{Z}$ and the open-circuit radiation patterns for the $Q+1$ ports $\mathbf{E}_{\text{oc}}$ can be obtained by performing only one EM simulation. Such one EM simulation contains $(Q+1)$ sub-simulations, so that each port will be sequentially excited and simulated in each sub-simulation. Thus, the total computational time to obtain $\mathbf{Z}$ and $\mathbf{E}_{\text{oc}}$ (including sequentially exciting each port in each sub-simulation) is 12 minutes.
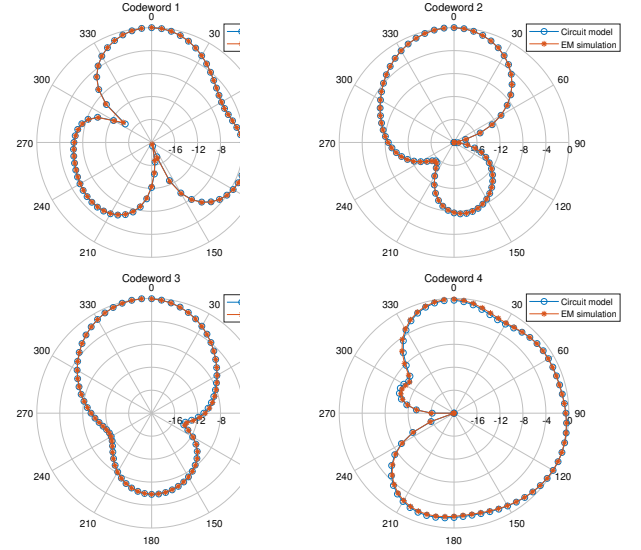

Fig. 11. Radiation patterns of the pixel antenna (with physical aperture $0.5\lambda \times 0.5\lambda$) configured by antenna coders in the codebook (with codebook size of 4) using EM simulation and multiport circuit network model. Unit: dB.

Second, when using the codebook to optimize the antenna coder, we need to design the codebook, which needs $N_c = N_o \left(\sum_{m=1}^{M} N_{e,m} 2^J \right)$ calculations of radiation pattern, where N_o is the number of iterations of antenna coder optimization in GLA and $N_{e,m}$ is the number of iterations for using SEBO to optimize the mth antenna coder in codebook with size of M. Once the codebook is ready, we search the codebook by M calculations of radiation pattern. Totally, we need $N_c + M$ calculations of radiation pattern to use codebook to optimize antenna coder, so the total computational time for the proposed multiport circuit network model is

$$T_{\text{total,circuit}} = T_0 + \left(N_o \left(\sum_{m=1}^{M} N_{e,m} 2^J \right) + M \right) T_{\text{circuit}}, \quad (67)$$

while the total computational time using EM simulation is

$$T_{\text{total,EM}} = \left(N_o \left(\sum_{m=1}^{M} N_{e,m} 2^J \right) + M \right) T_{\text{EM}}. \quad (68)$$

If considering $N_o = 1$ (the least number to perform antenna coding optimization in GLA), $N_{e,m} = 4 \ \forall m$, and e.g. $M = 16$, we have $T_{\text{total,circuit}} = 755$ s and $T_{\text{total,EM}} = 3709587$ s.

From the above complete comparison, we have shown that the proposed multiport circuit network model is significantly more computationally efficient than the EM simulation.

VI. DISCUSSIONS AND FUTURE WORK

A. Continuous Antenna Coding

It is possible to continuously adjust the load impedance $z_{\text{L},q}$ to implement a continuous antenna coding. To that end, we can use variable reactive load, such as varactor, to replace the RF switch in the pixel antenna, so that $z_{\text{L},q}$ can be modeled as $z_{\text{L},q} = j x_{\text{L},q}$, where j is the imaginary unit and $x_{\text{L},q}$ is the continuous variable reactance. Accordingly, the continuous antenna coding design becomes a continuous

optimization problem, which is easier to solve and can provide better performance compared with the binary antenna coding. However, implementing the continuous antenna coding increases the circuit complexity to control the pixel antenna since continuous dc bias voltages are required. Therefore, there is a tradeoff between the circuit complexity, system performance, and difficulty for optimization.

B. Antenna Coding Optimization for More Scenarios

Antenna coding can be optimized for more scenarios in future research, including, but are not limited to, the following:

1) Multi-User MIMO Pixel Antenna System: We can jointly optimize the precoding, combining, and antenna coding at transmitter and users to enhance the signal-to-interference-plus-noise ratio to maximize the weighted sum rate.

2) OFDM MIMO Pixel Antenna System: We can derive the frequency dependent model for pixel antenna and subsequently jointly optimize the precoding at each carrier frequency and the antenna coding of pixel antenna to maximize the capacity.

3) Pixel Antenna System for Wireless Power Transfer: We can jointly optimize the waveform, beamforming, and antenna coding to maximize the output dc power.

C. Pixel Antenna Element Spacing

There is a limitation on the spacing between adjacent pixel antenna elements, which should be neither too small nor too large, as explained in the following.

1) Inter-Element Electromagnetic Interference: When the spacing is too small, mutual coupling between the pixel antennas will be high and degrade the performance. In this work, we address the inter-element electromagnetic interference (EMI) issue in the MIMO pixel antenna system through separating the pixel antennas by a suitable distance to suppress the mutual coupling. For example, we separate two pixel antennas with physical aperture $0.25\lambda \times 0.25\lambda$ and $0.5\lambda \times 0.5\lambda$ by half-wavelength and one wavelength, respectively. Moreover, we can extend the proposed multiport circuit network model to take the inter-element EMI issue into account. For example, we consider two closely placed pixel antennas, which can be modeled as a $(2Q+2)$-port circuit network characterized by a $(2Q+2) \times (2Q+2)$ impedance matrix $\mathbf{Z}$. Given the antenna coders for pixel antennas 1 and 2, denoted as $\mathbf{b}_1$ and $\mathbf{b}_2$, we can find the corresponding load impedance $\mathbf{Z}_{\mathrm{L},1}(\mathbf{b}_1)$ and $\mathbf{Z}_{\mathrm{L},2}(\mathbf{b}_2)$. Thus, from $\mathbf{Z}$, $\mathbf{Z}_{\mathrm{L},1}(\mathbf{b}_1)$, and $\mathbf{Z}_{\mathrm{L},2}(\mathbf{b}_2)$, we can find the currents $\mathbf{i}_1(\mathbf{b}_1, \mathbf{b}_2)$ and $\mathbf{i}_2(\mathbf{b}_1, \mathbf{b}_2)$ and radiation patterns $\mathbf{e}_1(\mathbf{b}_1, \mathbf{b}_2)$ and $\mathbf{e}_2(\mathbf{b}_1, \mathbf{b}_2)$ for pixel antennas 1 and 2. Using the beamspace channel model, we can link the radiation patterns to the channel, so that we can optimize $\mathbf{b}_1$ and $\mathbf{b}_2$ to enhance the performance. By this way, the inter-element EMI issue can be fully characterized and considered. However, the extended model implies that the radiation pattern of individual pixel antenna is jointly coded by all the antenna coders due to the EMI issue, making the model complicate and intractable and increasing the complexity for antenna coding optimization.

2) Spherical Wave: When the spacing is too large, it makes the MIMO pixel antenna system very large, so the assumption of plane wave that we use becomes inaccurate. In this work, we assume that pixel antenna element spacing is not too large, as mentioned above, so that the plane wave assumption is valid. Otherwise, the effect of spherical wave should be incorporated in beamspace channel model for MIMO pixel antenna systems.

D. Pixel Antenna System Prototyping

Various pixel antennas have been designed, prototyped, and experimented. For example, in [8] and [10], the experiments for the pixel antenna prototypes have verified that the pixel antennas can flexibly reconfigure the radiation pattern toward different directions. Considering a line-of-sight (LOS) channel scenario, such pixel antennas can be directly used to generate an adaptive beam toward the receiver to enhance the system performance such as channel gain. Thus, the experiments provided in [8] and [10] have preliminarily verified the advantages of pixel antenna system in a simple LOS scenario. However, the previous work [8] and [10] were investigated at the level of antenna hardware design and limited to LOS scenario. To overcome this limitation, in this work we propose antenna coding which considers the impact on wireless communication with multipath fading at the system level to enhance the performance. Thus, in future research, the proposed pixel antenna system can be prototyped similarly to [8] and [10], but needs more efforts in the signal processing to control the pixel antenna with the proposed antenna coding technique.

VII. CONCLUSIONS

In this paper, we propose a novel technique denoted antenna coding empowered by pixel antennas. Pixel antennas are a flexible reconfigurable antenna technology based on discretizing a continuous radiation surface into small elements termed pixels. The characteristics of the pixel antennas, such as radiation patterns can be controlled by adjusting the connections between adjacent pixels through switches, which can be leveraged to enhance wireless communication systems.

We first derive a physical and EM based communication model for pixel antennas using microwave multiport network theory and beamspace channel representation. With the communication model, we consider the SISO pixel antenna system and optimize antenna coding using the SEBO algorithm to maximize channel gain. To lower computational complexity, we propose a codebook design for antenna coding based on the generalized Lloyd algorithm. We also analyze the average channel gain of SISO pixel antenna systems and derive that the upper bound of average channel gain is given by the EADoF of the pixel antennas. In addition, we jointly optimize the antenna coding and transmit signal covariance matrix to maximize the channel capacity in MIMO pixel antenna systems.

We evaluate the performance of SISO and MIMO pixel antenna systems compared to conventional SISO and MIMO systems. It is shown that using pixel antennas can enhance the average channel gain by up to 5.4 times and the channel capacity by up to 3.1 times, demonstrating the significant potential of pixel antennas as a new dimension to the design and optimization of wireless communication systems.

References

[1] Z. Wang, J. Zhang, H. Du, D. Niyato, S. Cui, B. Ai, M. Debbah, K. B. Letaief, and H. V. Poor, "A tutorial on extremely large-scale MIMO for 6G: Fundamentals, signal processing, and applications," *IEEE Commun. Surv. Tuts.*, vol. 26, no. 3, pp. 1560–1605, 2024.

[2] B. Cetiner, H. Jafarkhani, J.-Y. Qian, H. J. Yoo, A. Grau, and F. De Flaviis, "Multifunctional reconfigurable MEMS integrated antennas for adaptive MIMO systems," *IEEE Commun. Mag.*, vol. 42, no. 12, pp. 62–70, 2004.

[3] L. Pringle, P. Harms, S. Blalock, G. Kiesel, E. Kuster, P. Friederich, R. Prado, J. Morris, and G. Smith, "A reconfigurable aperture antenna based on switched links between electrically small metallic patches," *IEEE Trans. Antennas Propag.*, vol. 52, no. 6, pp. 1434–1445, 2004.

[4] A. Grau Besoli and F. De Flaviis, "A multifunctional reconfigurable pixeled antenna using MEMS technology on printed circuit board," *IEEE Trans. Antennas Propag.*, vol. 59, no. 12, pp. 4413–4424, 2011.

[5] D. Rodrigo and L. Jofre, "Frequency and radiation pattern reconfigurability of a multi-size pixel antenna," *IEEE Trans. Antennas Propag.*, vol. 60, no. 5, pp. 2219–2225, 2012.

[6] D. Rodrigo, B. A. Cetiner, and L. Jofre, "Frequency, radiation pattern and polarization reconfigurable antenna using a parasitic pixel layer," *IEEE Trans. Antennas Propag.*, vol. 62, no. 6, pp. 3422–3427, 2014.

[7] S. Song and R. D. Murch, "An efficient approach for optimizing frequency reconfigurable pixel antennas using genetic algorithms," *IEEE Trans. Antennas Propag.*, vol. 62, no. 2, pp. 609–620, Feb. 2014.

[8] P. Lotfi, S. Soltani, and R. D. Murch, "Printed endfire beam-steerable pixel antenna," *IEEE Trans. Antennas Propag.*, vol. 65, no. 8, pp. 3913–3923, 2017.

[9] Y. Zhang, Z. Han, S. Tang, S. Shen, C.-Y. Chiu, and R. Murch, "A highly pattern-reconfigurable planar antenna with 360° single- and multi-beam steering," *IEEE Trans. Antennas Propag.*, vol. 70, no. 8, pp. 6490–6504, 2022.

[10] Y. Zhang, S. Tang, Z. Han, J. Rao, S. Shen, M. Li, C.-Y. Chiu, and R. Murch, "A low-profile microstrip vertically polarized endfire antenna with 360° beam-scanning and high beam-shaping capability," *IEEE Trans. Antennas Propag.*, vol. 70, no. 9, pp. 7691–7702, 2022.

[11] J. Rao, Y. Zhang, S. Tang, Z. Li, S. Shen, C.-Y. Chiu, and R. Murch, "A novel reconfigurable intelligent surface for wide-angle passive beamforming," *IEEE Trans. Microw. Theory Techn.*, vol. 70, no. 12, pp. 5427–5439, 2022.

[12] S. Shen, C. Y. Chiu, and R. D. Murch, "Multiport pixel rectenna for ambient RF energy harvesting," *IEEE Trans. Antennas Propag.*, vol. 66, no. 2, pp. 644–656, Feb. 2018.

[13] S. Shen, Y. Zhang, C.-Y. Chiu, and R. Murch, "Directional multiport ambient RF energy-harvesting system for the internet of things," *IEEE Internet Things J.*, vol. 8, no. 7, pp. 5850–5865, 2021.

[14] Y. Zhang, S. Shen, Z. Han, C.-Y. Chiu, and R. Murch, "Compact MIMO systems utilizing a pixelated surface: Capacity maximization," *IEEE Trans. Veh. Technol.*, vol. 70, no. 9, pp. 8453–8467, 2021.

[15] Y. Zhang, Z. Han, S. Shen, C.-Y. Chiu, and R. Murch, "Polarization enhancement of microstrip antennas by asymmetric and symmetric grid defected ground structures," *IEEE Open J. Antennas Propag.*, vol. 1, pp. 215–223, 2020.

[16] K. K. Wong, A. Shojaeifard, K.-F. Tong, and Y. Zhang, "Performance limits of fluid antenna systems," *IEEE Commun. Lett.*, vol. 24, no. 11, pp. 2469–2472, 2020.

[17] Y. Huang, L. Xing, C. Song, S. Wang, and F. Elhouni, "Liquid antennas: Past, present and future," *IEEE Open J. Antennas Propag.*, vol. 2, pp. 473–487, 2021.

[18] J. Zhang, J. Rao, Z. Ming, Z. Li, C.-Y. Chiu, K.-K. Wong, K.-F. Tong, and R. Murch, "A pixel-based reconfigurable antenna design for fluid antenna systems," *arXiv preprint arXiv:2406.05499*, 2024.

[19] K.-K. Wong, A. Shojaeifard, K.-F. Tong, and Y. Zhang, "Fluid antenna systems," *IEEE Trans. Wireless Commun.*, vol. 20, no. 3, pp. 1950–1962, 2021.

[20] C. Psomas, G. M. Kraidy, K.-K. Wong, and I. Krikidis, "On the diversity and coded modulation design of fluid antenna systems," *IEEE Trans. Wireless Commun.*, vol. 23, no. 3, pp. 2082–2096, 2024.

[21] W. K. New, K.-K. Wong, H. Xu, K.-F. Tong, and C.-B. Chae, "Fluid antenna system: New insights on outage probability and diversity gain," *IEEE Trans. Wireless Commun.*, vol. 23, no. 1, pp. 128–140, 2024.

[22] ——, "An information-theoretic characterization of MIMO-FAS: Optimization, diversity-multiplexing tradeoff and q-outage capacity," *IEEE Trans. Wireless Commun.*, vol. 23, no. 6, pp. 5541–5556, 2024.

[23] W. Ma, L. Zhu, and R. Zhang, "MIMO capacity characterization for movable antenna systems," *IEEE Trans. Wireless Commun.*, vol. 23, no. 4, pp. 3392–3407, 2024.

[24] J. Zheng, J. Zhang, H. Du, D. Niyato, S. Sun, B. Ai, and K. B. Letaief, "Flexible-position MIMO for wireless communications: Fundamentals, challenges, and future directions," *IEEE Wireless Commun.*, pp. 1–9, 2024.

[25] Y. Ye, L. You, J. Wang, H. Xu, K.-K. Wong, and X. Gao, "Fluid antenna-assisted MIMO transmission exploiting statistical CSI," *IEEE Commun. Lett.*, vol. 28, no. 1, pp. 223–227, 2024.

[26] K.-K. Wong and K.-F. Tong, "Fluid antenna multiple access," *IEEE Trans. Wireless Commun.*, vol. 21, no. 7, pp. 4801–4815, 2022.

[27] K.-K. Wong, K.-F. Tong, Y. Chen, and Y. Zhang, "Fast fluid antenna multiple access enabling massive connectivity," *IEEE Commun. Lett.*, vol. 27, no. 2, pp. 711–715, 2023.

[28] K.-K. Wong, D. Morales-Jimenez, K.-F. Tong, and C.-B. Chae, "Slow fluid antenna multiple access," *IEEE Trans. Commun.*, vol. 71, no. 5, pp. 2831–2846, 2023.

[29] B. Tang, H. Xu, K.-K. Wong, K.-F. Tong, Y. Zhang, and C.-B. Chae, "Fluid antenna enabling secret communications," *IEEE Commun. Lett.*, vol. 27, no. 6, pp. 1491–1495, 2023.

[30] C. Skouroumounis and I. Krikidis, "Fluid antenna-aided full duplex communications: A macroscopic point-of-view," *IEEE J. Sel. Areas Commun.*, vol. 41, no. 9, pp. 2879–2892, 2023.

[31] J. Johnson and Y. Rahmat-Samii, "Genetic algorithms and method of moments (GA/MOM) for the design of integrated antennas," *IEEE Trans. Antennas Propag.*, vol. 47, no. 10, pp. 1606–1614, 1999.

[32] J. Perruisseau-Carrier, F. Bongard, R. Golubovic-Niciforovic, R. Torres-Sanchez, and J. R. Mosig, "Contributions to the modeling and design of reconfigurable reflecting cells embedding discrete control elements," *IEEE Trans. Microwave Theory Tech.*, vol. 58, no. 6, pp. 1621–1628, 2010.

[33] M. Yousefbeiki and J. Perruisseau-Carrier, "A practical technique for accurately modeling reconfigurable lumped components in commercial full-wave solvers [EurAAP corner]," *IEEE Antennas Propag. Mag.*, vol. 54, no. 5, pp. 298–303, 2012.

[34] J. Leonardo Araque Quijano and G. Vecchi, "Optimization of an innovative type of compact frequency-reconfigurable antenna," *IEEE Trans. Antennas Propag.*, vol. 57, no. 1, pp. 9–18, 2009.

[35] D. H. Johnson and E. Dan, "Array signal processing," 1993.

[36] A. Kalis, A. G. Kanatas, and C. B. Papadias, *Parasitic antenna arrays for wireless MIMO systems.* Springer, 2014.

[37] Z. Zhang, J. Zhu, L. Dai, and R. W. Heath Jr, "Successive bayesian reconstructor for channel estimation in flexible antenna systems," *arXiv preprint arXiv:2312.06551*, 2023.

[38] S. Shen, C. Y. Chiu, and R. D. Murch, "Optimization of 2.45-GHz pixel rectenna for wireless power transmission using mixed integer linear programming," in *Proc. IEEE Int. Symp. Antennas Propag. USNC/URSI Nat. Radio Sci. Meeting*, July 2017, pp. 351–352.

[39] F. Jiang, C.-Y. Chiu, S. Shen, Q. S. Cheng, and R. Murch, "Pixel antenna optimization using N-port characteristic mode analysis," *IEEE Trans. Antennas Propag.*, vol. 68, no. 5, pp. 3336–3347, 2020.

[40] F. Jiang, Z. Zhang, M. Li, S. Shen, C.-Y. Chiu, Y. Zhang, Q. S. Cheng, and R. Murch, "Multiport pixel antenna optimization using characteristic mode analysis and sequential feeding port search," *IEEE Trans. Antennas Propag.*, vol. 70, no. 10, pp. 9160–9174, 2022.

[41] F. Jiang, S. Shen, C.-Y. Chiu, Z. Zhang, Y. Zhang, Q. S. Cheng, and R. Murch, "Pixel antenna optimization based on perturbation sensitivity analysis," *IEEE Trans. Antennas Propag.*, vol. 70, no. 1, pp. 472–486, 2022.

[42] T. Qiao, F. Jiang, S. Shen, Z. Zhang, M. Li, C.-Y. Chiu, Q. S. Cheng, and R. Murch, "Pixel antenna optimization using the adjoint method and the method of moving asymptote," *IEEE Trans. Antennas Propag.*, vol. 71, no. 3, pp. 2873–2878, 2023.

[43] H. Chen, S. Li, Z. Wu, L. Wang, X.-C. Li, and Q. H. Liu, "Multi-head discrete action calibration proximal policy optimization method for pixel antennas with high degrees of freedom," *IEEE Trans. Antennas Propag.*, pp. 1–1, 2024.

[44] S. Shen, Y. Sun, S. Song, D. P. Palomar, and R. D. Murch, "Successive boolean optimization of planar pixel antennas," *IEEE Trans. Antennas Propag.*, vol. 65, no. 2, pp. 920–925, Feb. 2017.

[45] A. Gersho and R. M. Gray, *Vector quantization and signal compression.* Springer Science & Business Media, 2012, vol. 159.

[46] A. Shapiro, D. Dentcheva, and A. Ruszczynski, *Lectures on stochastic programming: modeling and theory.* SIAM, 2021.

[47] P. Xia and G. B. Giannakis, "Design and analysis of transmit-beamforming based on limited-rate feedback," *IEEE Trans. Signal Processing*, vol. 54, no. 5, pp. 1853–1863, 2006.

[48] Z. Han, Y. Zhang, S. Shen, Y. Li, C.-Y. Chiu, and R. Murch, "Characteristic mode analysis of ESPAR for single-RF MIMO systems," *IEEE Trans. Wireless Commun.*, vol. 20, no. 4, pp. 2353–2367, 2021.

[49] D. Tse and P. Viswanath, *Fundamentals of wireless communication*. Cambridge university press, 2005.